

# The Mount Pavagadh volcanic suite, Deccan Traps: Geochemical stratigraphy and magmatic evolution

Hetu C. Sheth<sup>a,\*</sup>, Leone Melluso<sup>b</sup>

<sup>a</sup> Department of Earth Sciences, Indian Institute of Technology (IIT) Bombay, Powai, Mumbai 400 076, India

<sup>b</sup> Dipartimento di Scienze della Terra, Università di Napoli Federico II, Via Mezzocannone 8, 80134 Napoli, Italy

Received 7 March 2007; received in revised form 24 August 2007; accepted 3 October 2007

## Abstract

The patterns of eruption and dispersal of flood basalt lavas on the surface, or as magmas in dykes and sills within the crust, determine the volcanological and stratigraphic development of flood basalt provinces. This is a geochemical and Sr-isotopic study of lavas of varied compositions that outcrop around Mount Pavagadh (829 m), Deccan Traps, an important outlier north of the main basalt outcrop. Most of the ~550-m thick exposed section at Pavagadh is made up of subalkalic basalts rich in the incompatible elements (particularly Nb, Ba, and Sr). Picrite and rhyolite–dacite flows also occur, the latter capping the sequence. The relatively high initial  $^{87}\text{Sr}/^{86}\text{Sr}$  ratios (up to 0.7083) and chemical characteristics of the rhyolitic rocks of Pavagadh are consistent with a small but significant involvement of the granitic basement crust in their genesis. An assimilation–fractional crystallization (AFC) model involving the picrite lava and either a southern Indian or a western Indian granite as the contaminant explains the geochemical and Sr-isotopic variation in the basalts and the rhyolites quite well. A systematic comparison of the basaltic lavas (with binary plots, normalized multielement patterns, and discriminant function analysis) to the well-established lava stratigraphy of the Western Ghats, 400–500 km to the south, precludes any chemical–genetic relationships between the two. Basalts exposed in sections closer to Pavagadh (~150–200 km), in the Toranmal, Navagam, and Barwani–Mhow areas, have several flows with some similar chemical characteristics. However, the Pavagadh sequence is significantly different from all of these sequences geochemically, petrogenetically, and in magnetic polarity, to be considered independently built. This result is significant in terms of eruptive models for the Deccan Traps, as it is increasingly apparent that there were separate but possibly coeval eruptive centers with their own distinctive chemistries developed in various areas of this vast province.

© 2007 Elsevier Ltd. All rights reserved.

**Keywords:** Volcanism; Magma; Lava; Flood basalt; Rhyolite; Deccan Traps; India

## 1. Introduction

Continental flood basalt (CFB) provinces are vast and thick accumulations of tholeiitic basalt lavas, and often also include variable volumes of alkalic and silicic rocks (e.g., Macdougall, 1988; Mahoney and Coffin, 1997). The Karoo, the Paraná, and the Deccan CFB provinces are good examples. The lavas are also usually horizontally disposed over vast areas, and the techniques of geochemical

and magnetic stratigraphy – long-distance correlation of lavas and lava piles based on their geochemical signatures and magnetic polarity – have been successfully used to understand the stratigraphic and structural make-up of these provinces (e.g., Peate, 1997; Marsh et al., 1997). The genesis of the silicic (rhyolitic–dacitic–trachytic) magmas in CFBs is also of considerable petrogenetic interest. These have been variably interpreted as products of fractional crystallization of mafic magmas, combined assimilation and fractional crystallization, partial melting of underplated mafic rocks or deep basaltic piles, partial melting of pre-existing altered rhyolites, or anatexis of the continental crust (e.g., Betton, 1979; Bellieni et al., 1984;

\* Corresponding author. Tel.: +91 22 25767264; fax: +91 22 25767253.  
E-mail address: [hesheth@iitb.ac.in](mailto:hesheth@iitb.ac.in) (H.C. Sheth).

Garland et al., 1995; Lightfoot et al., 1987; Sheth and Ray, 2002; Miller and Harris, 2007).

The addition of flood basalt magmas to the crust, via dykes or sills, and their transport as lavas after eruption, is of interest and significance to understand the physical growth and stratigraphic development of such huge flood basalt provinces (e.g., Bondre et al., 2006; Sheth, 2006; Vanderkluyzen et al., 2006; Ray et al., 2007). The Deccan, a magnificent CFB province exposed in western and central India, covers  $\sim 500,000 \text{ km}^2$  after some 65 million years of erosion, and a considerable area lies submerged in the Arabian Sea to the west (Fig. 1). The Deccan CFB pile is best exposed in the Western Ghats (Sahyadri) range in the southwest of the province (Fig. 1), where a stratigraphic thickness of  $\sim 3 \text{ km}$  has been divided into various formations and subgroups (Table 1) (e.g., Cox and Hawkesworth, 1985; Beane et al., 1986; see Subbarao and Hooper, 1988). Several workers (e.g., Sreenivasa Rao et al., 1985; Mitchell and Widdowson, 1991; Dhandapani and Subbarao, 1992; Peng et al., 1998; Bilgrami, 1999; Mahoney et al., 2000; Sheth et al., 2004a) have attempted long-distance geochemical correlations of thick basalt sections in the province with the Western Ghats sequence with the aim to develop suitable eruptive models.

## 2. The Pavagadh section and its significance

The imposing mountain of Pavagadh (829 m, Fig. 1), rising nearly 700 m above the surrounding plains, constitutes an important lava sequence in the Deccan Traps. It is separated from the main Deccan outcrop by post-Deccan tertiary and quaternary alluvium and a complex Precambrian basement made up of granites, gneisses, and quartzites. Pavagadh shows a  $\sim 550\text{-m}$  thick exposed sequence made up of perfectly horizontal flood basalt lavas and rhyolitic lavas, the latter at the top. Pavagadh is of particular interest because of the following reasons:

- (1) A study on the geochemical stratigraphy of the Pavagadh sequence, and regional stratigraphic correlations have not yet been attempted.
- (2) The petrogenesis of particularly the rhyolitic rocks capping the sequence, as well as a couple of picritic lavas, is of considerable interest.
- (3) The Pavagadh sequence is a rare bimodal lava sequence in the Deccan, akin to many present in the Paraná and Karoo provinces (e.g., Peate, 1997).
- (4) The eruptive areas of the lava sequence are unknown; the nearest dykes and mafic and silicic intrusions are exposed some 50–75 km to the south, in the Narmada River region around Rajpipla and Navagam (Fig. 1; Krishnamurthy and Cox, 1980; Mahoney et al., 1985). Recent and ongoing dyke-flow correlation work in the province (Widdowson et al., 2000; Bondre et al., 2006; Vanderkluyzen et al., 2006 and in preparation) builds on a large amount of high-quality geochemical data (including Sr–Nd–Pb isotopes) for both lava sequences and dyke swarms.
- (5) A N–R–N magnetic polarity stratigraphy (i.e., two magnetic reversals) has been unambiguously documented from sampled sections between Barwani and Mhow, in the Satpura–Narmada region (Fig. 1; e.g., Sreenivasa Rao et al., 1985; Dhandapani and Subbarao, 1992). Most of the thick Western Ghats lava sequence is reversely magnetized, with only the Mahabaleshwar and Panhala formations being normally magnetized (Table 1). Interestingly, the lava pile forming the upper two-thirds of Mount Pavagadh is normally magnetized, whereas the lower one third yielded random directions (Verma and Mittal, 1974). If, thus, the normally polarized lavas of Pavagadh are neither geochemical nor stratigraphic equivalents of the normally magnetized lavas at the top of the Western Ghats (the Mahabaleshwar and Panhala formations), then these Pavagadh lavas must stratigraphically correspond to the older Normal chron recorded in sections located 150–200 km away in the Satpura–Narmada region, and like the latter the Pavagadh lavas must be *older than* the whole exposed Western Ghats stratigraphy.

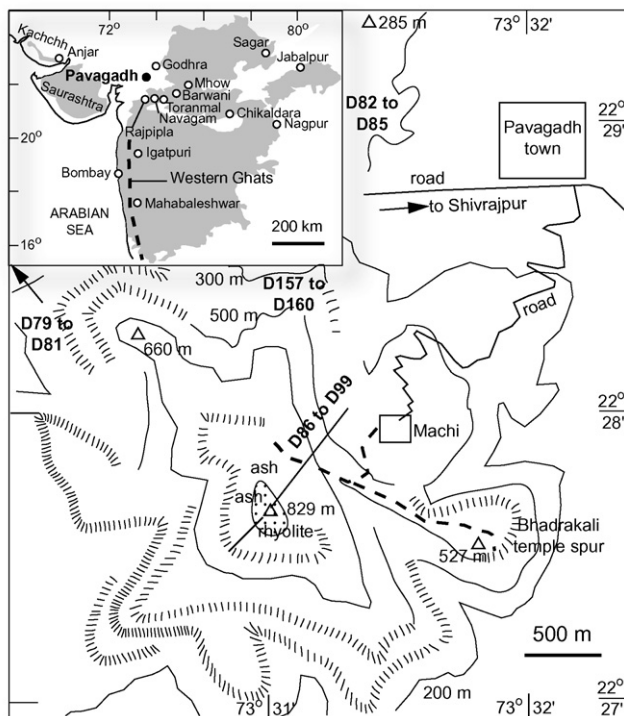


Fig. 1. Topographic sketch-map of Mount Pavagadh, modified from Sheth et al. (2004b) and with the sample locations added (see Table 1 for exact elevations of samples). Fence-like linear patterns mark near-vertical cliffs. The pilgrim route from Machi to the summit is shown as a dashed line. Inset shows the outcrop of the Deccan flood basalt province (shaded), and the locations of Pavagadh and other sections discussed in the text.

Table 1  
Stratigraphy of the Deccan flood basalts in the Western Ghats, with formation thicknesses, magnetic polarity, and Sr isotopic values (at 66 Ma)

Group	Sub-group	Formation	Magnetic polarity	$^{87}\text{Sr}/^{86}\text{Sr}_{(66\text{Ma})}$
Deccan Basalt	Wai	Desur <sup>a</sup> (~100 m)	N	0.7072–0.7080
		Panhala (>175 m)	N	0.7046–0.7055
		Mahabaleshwar (280 m)	N	0.7040–0.7055
		Ambenali (500 m)	R	0.7038–0.7044
		Poladpur (375 m)	R	0.7053–0.7110
	Lonavala	Bushe (325 m)	R	0.7078–0.7200
		Khandala (140 m)	R	0.7071–0.7124
	Kalsubai	Bhimashankar (140 m)	R	0.7067–0.7076
		Thakurvadi (650 m)	R	0.7067–0.7112
		Neral (100 m)	R	0.7062–0.7104
		Igatpuri-Jawhar (>700 m)	R	0.7085–0.7128

<sup>a</sup> The Desur is considered by many as a “Unit” of the Panhala formation itself. Table based on Sreenivasa Rao et al. (1985) and references therein, and Peng et al. (1994). *N* = normal magnetic polarity, *R* = reversed magnetic polarity.

Here, major and trace element and Sr-isotopic data on the Pavagadh suite of rocks are presented, and their implications for petrogenesis and magmatic evolution as well as the regional stratigraphy of the Deccan Traps are discussed.

### 3. Field work and samples

The lava pile of Mount Pavagadh is exposed between ~300 m and 829 m above MSL. No unambiguously in situ outcrops are found in the jungle on the lower slopes of the mountain below Machi (Fig. 1) at ~300 m elevation. The lavas were sampled along the pilgrim path from Machi to the Hindu shrine at the summit, and also in the hills and quarries north and northwest of the mountain, where stratigraphic relationships are very ambiguous. The elevation of each sample taken on the mountain was noted with an altimeter with a precision of  $\pm 10$  m. Unfortunately, exposure is poor even along the pilgrim path due to construction, the outcrops significantly weathered, and flow boundaries rarely clear. Below Machi, large blocks of rhyolitic rocks are found on the side of the road, and whether they represent boulders of the top rhyolite fallen from the summit, or mark a local rhyolite eruption in situ, is unknown.

The rhyolite flow at the top forms cliffs, and shows large, roughly vertical joints and curved sub-horizontal fractures, with some spectacular flow layering and flow folding. There is also a thin layer of pitchstone locally developed within the rhyolite, without sharp contacts. Fine, soft, friable rhyolitic ash (green or brown) is exposed below the rhyolite on the northwest side. Sheth et al. (2004b) reported, from the topmost mafic flow underlying the summit rhyolite and ash, low-relief circular cone-and-crater structures, which they considered as possible rootless cones formed in the basaltic flow as it would have advanced across a river or a lake.

### 4. Analytical methods

The samples were crushed into chips using a steel jaw crusher, and the chips were first washed in distilled water

and then ground in agate. Major and trace elements were analyzed at Naples (CISAG) with a Philips PW1400 X-ray fluorescence (XRF) spectrometer (see Melluso et al., 1995, 2004, 2005, 2006 for details). Precision is estimated at better than 1% for SiO<sub>2</sub>, TiO<sub>2</sub>, Al<sub>2</sub>O<sub>3</sub>, Fe<sub>2</sub>O<sub>3</sub><sup>\*</sup>, and CaO, better than 6% for K<sub>2</sub>O, 0.03 wt% for MnO and P<sub>2</sub>O<sub>5</sub>, and better than 5–10% for Sc, V, Cr, Ni, Cu, Ba, Zn, Sr, Y, and Zr for the observed ranges of concentration. Na and Mg were analyzed by atomic absorption spectrophotometry (AAS) at Naples, the precision being better than 6% for Na and better than 2% for Mg. The data are given in Table 2.

The rare earth elements and U, Th, Pb, Ta, and Hf were analyzed for a couple of samples by inductively coupled plasma mass spectrometry (ICPMS) at CRPG Nancy; precision is better than 5–10%. Microprobe analyses of minerals were performed at Cagliari University, using silicates and oxides as standards, an ARL-SEM-Q instrument and the MAGIC IV correction method. Strontium-isotopic compositions were measured at University of Rome, using a VG54E thermal ionization mass spectrometer; full analytical details can be found in Comin-Chiaramonti et al. (1997). Two samples were also analyzed for Nd–Sr–Pb isotopes at the University of Hawaii, following methods outlined in Mahoney et al. (2000) and Melluso et al. (2006). The trace element data are tabulated in Table 3, and Sr-isotopic ratios in Table 4.

### 5. Nomenclature, petrography, and mineral chemistry

Previous workers (e.g., Chatterjee, 1961; Hari et al., 2000; Furuyama et al., 2001) have used much non-standard terminology to describe the rock types (e.g., hawaiiite, mugearite, dellenite, and ankaramite), the use of which is no longer recommended (IUGS Subcommittee on the Systematics of Igneous Rocks, Le Bas et al., 1986; Le Bas, 2000). This study uses only the standardized terminology adopted by this Subcommittee and terms such as ankaramite are used in addition, where required. Table 2 shows the major element compositions (calculated on an anhydrous basis) and normative compositions of the suite,

Table 2  
Major oxide (wt%) and normative compositions of the Pavagadh volcanic suite

Sample	D86	D87	D88	D89	D99	D92	D93	D94	D95	D96	D97	D98
Location	829 m	800 m	770 m	770 m	765 m	705 m	685 m	665 m	645 m	580 m	565 m	480 m
Rock type	R	R	R	R	D	B, subal	PIC	B, subal				
SiO <sub>2</sub>	79.68	70.56	77.24	70.31	72.57	50.20	48.91	49.23	49.81	47.57	46.20	50.74
TiO <sub>2</sub>	0.35	0.69	0.41	0.67	0.63	2.67	2.96	2.83	3.19	2.43	2.49	2.67
Al <sub>2</sub> O <sub>3</sub>	10.01	13.79	11.05	13.29	13.53	16.66	17.02	16.97	14.30	13.78	13.45	15.06
Fe <sub>2</sub> O <sub>3</sub>	0.72	1.54	0.90	1.72	1.56	1.90	2.05	1.91	2.20	1.98	1.95	1.85
FeO	1.44	3.08	1.81	3.44	3.89	9.48	10.26	9.56	10.98	9.89	9.74	9.23
MnO	0.05	0.08	0.04	0.13	0.19	0.12	0.17	0.16	0.20	0.20	0.15	0.18
MgO	0.07	0.16	0.06	0.63	1.73	4.47	4.18	4.46	5.44	8.54	13.16	5.62
CaO	0.15	1.25	0.33	2.17	3.93	9.16	9.38	9.55	9.28	12.67	9.94	10.39
Na <sub>2</sub> O	1.64	3.40	2.09	4.37	0.90	3.12	3.15	3.22	2.87	2.11	1.77	2.62
K <sub>2</sub> O	5.87	5.33	6.04	3.18	0.98	1.69	1.47	1.56	1.44	0.62	0.80	1.40
P <sub>2</sub> O <sub>5</sub>	0.02	0.10	0.01	0.08	0.08	0.54	0.45	0.54	0.28	0.21	0.35	0.24
LOI	nd	0.91	0.96	2.01	8.31	nd	nd	nd	2.03	1.43	2.48	1.83
Mg#	7.96	8.47	5.58	24.6	44.1	45.6	42.1	45.4	46.9	60.6	70.7	52.0
Q	46.57	26.19	40.27	26.18	50.43	–	–	–	–	–	–	0.36
Or	34.69	31.49	35.71	18.80	5.81	9.97	8.67	9.20	8.50	3.65	4.72	8.30
Ab	13.90	28.79	17.72	36.94	7.65	26.43	26.62	27.29	24.33	17.88	14.98	22.14
An	0.61	5.57	1.58	7.26	18.96	26.45	27.98	27.24	21.88	26.29	26.39	25.21
C	0.72	0.38	0.49	–	4.03	–	–	–	–	–	–	–
Di	–	–	–	2.53	–	12.83	12.97	13.80	18.47	28.63	16.57	20.33
Hy	1.74	3.79	2.12	4.31	9.47	11.96	7.25	5.29	14.34	3.16	7.59	15.35
Ol	–	–	–	–	–	3.29	6.85	7.79	2.59	12.42	21.39	–
Mt	1.04	2.24	1.31	2.50	2.26	2.75	2.97	2.77	3.18	2.87	2.82	2.68
Il	0.66	1.31	0.78	1.28	1.20	5.07	5.63	5.38	6.06	4.61	4.72	5.07
Ap	0.05	0.23	0.02	0.18	0.18	1.24	1.05	1.24	0.66	0.49	0.82	0.56

Sample	D157	D158	D159	D160	D79	D81	D80	D85	D84	D82	D83	W2	W2
Location	390 m	390 m	355 m	325 m	NWP	NWP	NWP	NP	NP	NP	NP	Std.	Std.
Rock type	B, subal	PIC	B, subal	B, subal	B, subal	PIC	B, subal	Meas.	Ref.				
SiO <sub>2</sub>	48.73	50.77	51.12	46.35	48.75	46.31	51.84	48.94	48.20	44.97	48.00	52.50	52.68
TiO <sub>2</sub>	2.56	3.10	2.74	3.53	2.90	1.92	2.90	2.93	3.37	2.36	2.91	1.03	1.06
Al <sub>2</sub> O <sub>3</sub>	16.04	13.96	14.57	17.75	16.49	11.98	14.45	17.12	14.82	11.57	15.49	15.57	15.45
Fe <sub>2</sub> O <sub>3</sub>	1.96	2.06	1.94	2.23	1.92	1.96	2.03	1.80	2.13	1.73	1.94	10.95*	10.79*
FeO	9.82	10.30	9.70	11.17	9.63	9.80	10.14	9.02	10.66	11.53	9.68	–	–
MnO	0.15	0.16	0.18	0.15	0.17	0.14	0.14	0.14	0.20	0.20	0.23	0.16	0.17
MgO	6.19	5.78	5.81	4.10	6.38	14.46	3.15	4.03	6.04	15.60	6.35	6.59	6.37
CaO	10.48	9.88	9.79	11.45	9.30	11.24	10.17	12.02	10.67	9.98	11.10	10.73	10.86
Na <sub>2</sub> O	2.64	2.58	2.72	1.52	2.92	1.29	3.54	2.32	2.60	1.21	2.73	2.29	2.20
K <sub>2</sub> O	1.04	1.17	1.18	1.32	1.25	0.63	1.43	1.21	1.07	0.57	1.21	0.65	0.63
P <sub>2</sub> O <sub>5</sub>	0.38	0.23	0.24	0.42	0.28	0.27	0.21	0.46	0.22	0.27	0.35	0.17	0.14
LOI	nd	1.70	1.04	nd	2.84	2.84	2.31	nd	1.71	9.84	nd	–	–
Mg#	52.9	50.0	51.6	39.6	54.1	72.4	35.7	44.3	50.2	70.7	53.9	–	–
Q	–	1.784	1.284	0.581	–	–	0.667	0.712	–	–	–	–	–
Or	6.16	6.93	6.99	7.78	7.40	3.70	8.43	7.16	6.34	3.35	7.17	–	–
Ab	22.33	21.82	23.01	12.85	24.72	10.95	29.95	19.66	22.01	10.20	23.09	–	–
An	28.84	23.04	24.04	37.72	28.19	25.02	19.32	32.71	25.61	24.48	26.45	–	–
C	–	–	–	–	–	–	–	–	–	–	–	–	–
Di	16.95	20.13	18.89	13.59	13.17	23.27	25.00	19.79	21.26	18.72	21.55	–	–
Hy	10.48	16.86	17.21	16.53	8.10	8.40	7.69	10.71	8.06	8.46	0.46	–	–
Ol	6.64	–	–	–	9.46	21.52	–	–	6.70	27.15	12.12	–	–
Mt	2.85	2.98	2.81	3.24	2.79	2.84	2.94	2.61	3.09	2.51	2.81	–	–
Il	4.86	5.90	5.20	6.71	5.51	3.65	5.51	5.56	6.40	4.48	5.53	–	–
Ap	0.89	0.54	0.56	0.98	0.66	0.63	0.49	1.08	0.52	0.63	0.82	–	–

Notes: NWP = northwest of Pavagadh; NP = north of Pavagadh; R = rhyolite, D = dacite, B, subal = basalt (sub-alkalic), PIC = picrite. D89 is a pitchstone underlain by D88. D158 is just below D157. D160 is auto-brecciated lava flow just below D159. Normative compositions and the major oxide data (recalculated on an anhydrous basis, and Fe<sub>2</sub>O<sub>3</sub>T separated into Fe<sub>2</sub>O<sub>3</sub> and FeO) obtained using the SINCLAS program of Verma et al. (2002). For standard W-2, values with the asterisk \* mean Fe<sub>2</sub>O<sub>3</sub>T. “Meas” are the measured values, and “Ref” are the reference values recommended by Govindaraju (1989). LOI is reported where available and provides an idea of the sub-aerial alteration suffered by the rocks. nd = not determined. Mg# = [atomic Mg/(Mg+Fe<sup>2+</sup>)] × 100, assuming Fe<sup>3+</sup>/Fe<sup>2+</sup> = 0.16.

Table 3  
Trace element data for the Pavagadh volcanic suite

Sample	D86	D87	D88	D89	D99	D92	D93	D94	D95	D96	D97	D98	D157	D158	D159	D160	D79	D81	D80	D85	D84	D82	D83	W2	W2
Elev. (m)	829	800	770	770	765	705	685	665	645	580	565	480	390	390	355	325	NWP	NWP	NWP	NP	NP	NP	NP	Std.	Std.
Rock type	R	R	R	R	D	B	B	B	B	B	PIC	B	B	B	B	B	B	PIC	B	B	B	PIC	B	M	R
Sc				10	12					41	28			30			24	36				27		31	35
V	4	17	15	3	14	368	391	380	429	423	249	353		455	451	311	294	255	368	255	437	287	369	235	262
Cr	4			3		23	23	20	42	174	819	40	178	106	47	58	6	952.2	64	136	48	951	155	90	93
Ni		9		6		15	14	12	28	128	381	48	124	81	49	71	50	400.1	49	81	82	421	77	70	70
Zn	51		78	113	128	104	114	99	129	101	98	97	95	131	111	128	99	87	134	101	123	89	107	78	77
Rb	192	190	214	189	46	42	39	38	29	12	23	33	29	22	16	34	18	46	22	23			26	24	20
Sr	77	165	50	192	1961	492	497	524	465	364	297	522	407	429	410	106	510	300	317	138	491		508	190	194
Y	48	61	62	63	112	34	33	34	38	26	21	27	27	37	33	31	27	21	27	32	33	18	27	21	24
Zr	154	552	451	536	458	235	230	229	250	161	160	172	184	232	216	203	186	121	127	235	225	135	204	94	94
Nb	40	60	59	60	45	42	39	39	52	30	26	36	27	37	37	37	33	20	42	63	57	25	43	6.8	7.9
Ba	345	875	472	947	1766	503	478	474	416	249	364	439		403	317	376	574	347	372	278	375		349	190	182
La				94.3	105						21.1			31.2			30.4	15.2				22			
Ce				178	210						50.1			72.8			59.5	33.8				41.7			
Pr				21.2							6.21							4.06							
Nd				77.2	92.8						25.1			36.2			29.9	17.4				20.8			
Sm				16.2	21.3						5.98			8.58			6.45	4.22				4.7			
Eu				3.49	4.17						1.75			2.58			2.13	1.32				1.63			
Gd				13.5	22.0						5.97			8.03			6.03	4.33				5			
Tb				1.77							0.72							0.53							
Dy				11.9	19.2						4.44			6.44			4.99	3.06				3.33			
Ho				2.17							0.83							0.53							
Er				5.48	10.3						2.06			3.01			2.27	1.36				1.26			
Tm				0.89							0.28							0.19							
Yb				5.51	9.86						1.7			2.48			2.01	1.09				1.26			
Lu				0.83	1.68						0.28			0.43			0.34	0.23				0.18			
Ta				4.42							2.10							1.40							
Pb				26							2.38							1.75							
Th				31.2							3.45			3.00			6.00	1.99							
U				7.18							0.65							0.34							

Notes: W2 "M" and W2 "R" are the measured and reference values (Govindaraju, 1989), respectively, for the standard W2.

Table 4  
Isotopic ratios age-corrected to 66 Ma for the Pavagadh volcanic suite

Sample	D87	D89	D96	D97	D79	D81
	R, 800 m	R, 770 m	B, 580 m	PIC, 565 m	B, NWP	PIC, NWP
$^{143}\text{Nd}/^{144}\text{Nd}(t)$				0.512759		0.512701
$\varepsilon_{\text{Nd}}(t)$				+4.0		+2.9
$^{87}\text{Sr}/^{86}\text{Sr}(t)$	0.70639	0.70826	0.70495	0.70450	0.70626	0.70444
						0.70458*
$^{206}\text{Pb}/^{204}\text{Pb}(t)$				18.796		18.608
$^{207}\text{Pb}/^{204}\text{Pb}(t)$				15.630		15.605
$^{208}\text{Pb}/^{204}\text{Pb}(t)$				39.064		38.879

Notes:  $\varepsilon_{\text{Nd}}(0) = 0$  today corresponds to  $^{143}\text{Nd}/^{144}\text{Nd} = 0.512640$ ;  $\varepsilon_{\text{Nd}}(t) = 0$  at 66 Ma corresponds to  $^{143}\text{Nd}/^{144}\text{Nd} = 0.512555$ . All Sr-isotopic work was at University of Rome, except for D81, where the ratio obtained at Rome (0.70458) differs slightly from that obtained at University of Hawaii (0.70444) by Melluso et al. (2006); the latter is preferred.

the latter obtained with the SINCLAS program of Verma et al. (2002), which has been developed to comply with IUGS nomenclature and also provides a standard rock name for each sample. The Middlemost (1989) option provided within SINCLAS was used for dividing the iron into ferrous and ferric iron. The Pavagadh data (Fig. 2) plot in the basalt and rhyolite fields, with one picrite and one dacite, on the total alkali–silica (TAS) diagram (Le Bas et al., 1986). Here, most data also plot below the alkalic–subalkalic boundary (heavy line) of Irvine and Baragar (1971), showing that most of the lavas are subalkalic (Fig. 2). Greenough et al. (1998) called the suite mildly alkalic, using plots such as the Zr–TiO<sub>2</sub> plot of Floyd and Winchester (1978). Not only does this plot show a large overlap between tholeiitic and alkali basalts, but Greenough et al.’s data points could belong to either category (see their Fig. 3). Most important, alkalic or subalkalic nature of volcanic rocks must be determined purely on the basis of total alkali and silica contents (see also Sheth et al., 2002). As seen in Fig. 2, the TAS diagram, most samples of Greenough et al. (1998) (recalculated on an anhy-

drous basis using SINCLAS) are subalkalic. All samples of the present study are hypersthene-normative (1.74–17.2%), and have variable normative olivine (up to 27.2%). The rhyolite and dacite are strongly quartz normative (up to 50.4% in the altered sample D99). Note that the samples D97 (three-phenocryst basalt) and D81 (ankaramite) each have MgO > 12 wt%, and therefore are picrites by the standard nomenclature (Le Bas, 2000). Both are olivine- and clinopyroxene-phyric, with plagioclase phenocrysts also abundant in D97. Olivine is usually altered, and often has chromite inclusions. The ankaramite D82 to the north of Pavagadh has also chromite, olivine, and clinopyroxene phenocrysts, and is highly altered (LOI = 9.84 wt%). Basalts are generally sparsely phyric, with phenocrysts of plagioclase, clinopyroxene and strongly altered olivine, in a pilotaxitic mesostasis rich in opaque microlites, in addition to plagioclase and clinopyroxene. The basalt D79 has fresh Fe-rich olivines and an ophitic texture with clinopyroxene enclosing olivine and plagioclase, interstitial opaques and, unusually, phlogopite.

The pitchstone (sample D89) is very fresh and sparsely phyric, with iddingsitized Fe-olivine, plagioclase, opaques, pigeonite, and augite phenocrysts and microphenocrysts in a glassy matrix. The tuffaceous rocks have textures similar to those of pyroclastic flow deposits. The rocks are sometimes crystal-rich (mostly plagioclase), and pumice fragments are frequently observed in the oriented, often devitrified, glassy matrix with flow textures. Representative analyses of the most important mineral phases found in the Pavagadh rocks are plotted in Fig. 3, and full data tables can be obtained from the authors. Olivine ranges from Fo<sub>88</sub> in the phenocryst cores in D97 to Fo<sub>49</sub> in the D79 mesostasis. The pitchstone D89 has rare uniformly Fe-rich olivines (Fo<sub>27</sub>–Fo<sub>28</sub>). Pyroxene in the basalts is Ca-rich, close to diopside-salite (Ca<sub>46</sub>Mg<sub>47</sub>Fe<sub>7</sub> to Ca<sub>46</sub>Mg<sub>27</sub>Fe<sub>27</sub>), with variable but generally high, TiO<sub>2</sub> (0.65–3.03 wt%). Fe-augite (Ca<sub>36</sub>Mg<sub>31</sub>Fe<sub>32</sub> to Ca<sub>46</sub>Mg<sub>27</sub>Fe<sub>27</sub>) and Fe-pigeonite (Ca<sub>9</sub>Mg<sub>37</sub>Fe<sub>54</sub> to Ca<sub>10</sub>Mg<sub>34</sub>Fe<sub>56</sub>) are present in the pitchstone D89. Basalt-groundmass feldspars range from An<sub>74</sub> to anorthoclase and sodic sanidine (Or<sub>52</sub>Ab<sub>42</sub>An<sub>6</sub>). Rhyolites have sodic plagioclase (An<sub>40</sub>) to anorthoclase (Ab<sub>64</sub>Or<sub>24</sub>An<sub>6</sub>). The phlogopite in the basalt D79 is Mg-

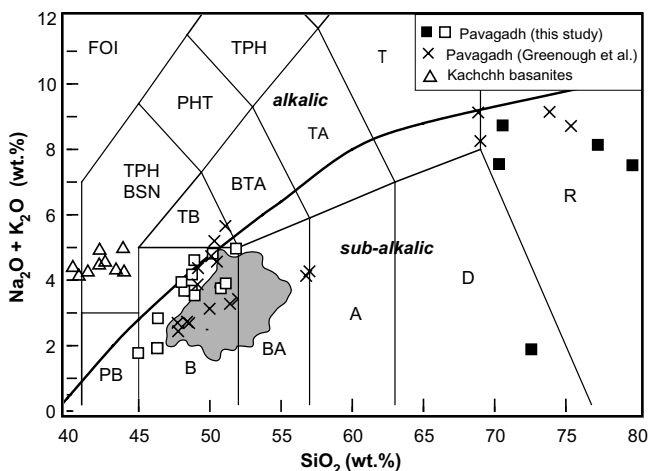


Fig. 2. The Pavagadh data (this study and Greenough et al., 1998) on the TAS diagram (Le Bas et al., 1986). The Western Ghats lavas (624 samples, Beane, 1988) are shown for comparison (shaded area), as are the basanites of Kachchh (Karmalkar et al., 2005). Curved line is the boundary between alkalic and subalkalic rocks proposed by Irvine and Baragar (1971).

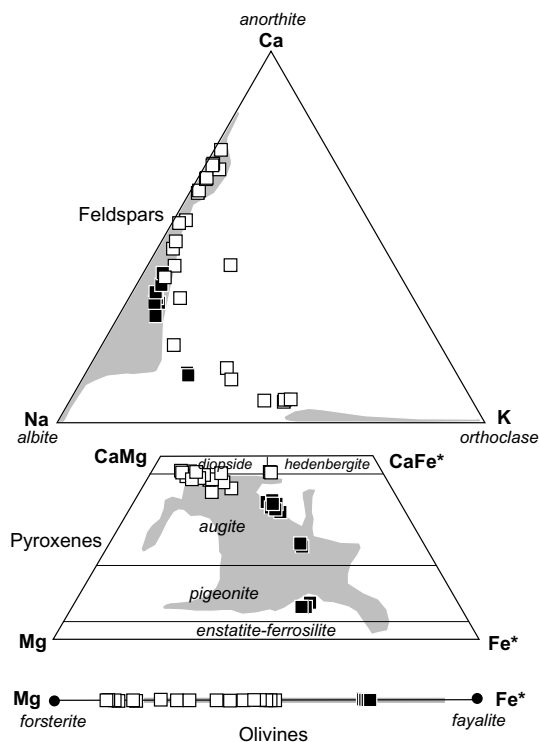


Fig. 3. Compositions of feldspars, pyroxenes and olivines in the Pavagadh suite of rocks. Open squares are the mafic and ultramafic rocks and black squares are the silicic rocks. Grey shaded areas cover the hundreds of unpublished analyses of L. Melluso from the Deccan province.

rich (21–22 wt% MgO) and has relatively high  $\text{TiO}_2$  (2.4–4.4 wt%).

The silicic pyroxenes of the Pavagadh basalts indicate a relatively alkaline affinity of the parental magmas, and differ from the typical Ca-rich pyroxenes (augitic-ferroaugitic) of the largely tholeiitic Deccan Traps (Fig. 3). This alkaline tendency is also noted from the presence of anorthoclase in the groundmass of the basalts and in the rhyolites. This is not to say that the Pavagadh lavas are alkalic (by normative composition or on the TAS diagram), of course. The presence of pigeonite in the rhyolites, and the complete absence of pigeonite in the basalts is also noteworthy. Fe–Ti oxides are present as Cr-rich spinels included in olivine, Ti-magnetites and ilmenites. The equilibration temperatures and oxygen fugacities (Fig. 4) calculated using magnetite-ilmenite analyses range from 1171 °C,  $10^{-8.82}$  bars  $f\text{O}_2$  to 863 °C,  $10^{-13.3}$  bars  $f\text{O}_2$  (X'Usp and X'Ilm recalculation methods given in LePage, 2003). In comparison, Hari et al. (1991) determined the higher-end range of 1040–1240 °C in the form of homogenization temperatures for olivine-hosted melt inclusions in some of these rocks (Hari et al., 1991).

## 6. Magmatic evolution

### 6.1. Partial melting

Melluso et al. (2006) have recently provided an elemental and isotopic study of the picritic or high-MgO

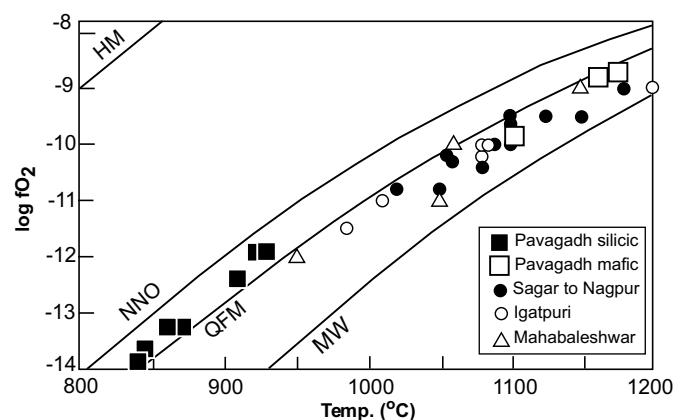


Fig. 4. Oxygen fugacity and Fe–Ti oxide equilibration temperatures for the Pavagadh silicic and mafic lavas. Shown for comparison are data of Sethna et al. (1987) for Deccan basalts of Sagar to Nagpur area (filled circles), Igatpuri section (open circles) and Mahabaleshwar section (open triangles). See Fig. 1 inset for locations. The four curves labeled HM, NNO, QFM, and MW represent the buffer curves haematite–magnetite, nickel–nickel oxide, quartz–fayalite–magnetite, and wüstite–magnetite, respectively (after Eugster and Wones, 1962).

( $\geq 10$  wt%) basalts and picrites of Gujarat, including the picritic lavas at Pavagadh (D97 and D81). Such high-MgO rocks (picrites and ankaramites) can be primitive (high-MgO) liquids formed by melting of mantle rocks at high temperature and pressure, which evolve to basaltic magmas by pronounced olivine  $\pm$  clinopyroxene fractionation (e.g., Cox, 1980). More commonly, they are the products of accumulation of olivine  $\pm$  clinopyroxene in basaltic liquids. Considerations of olivine-liquid and clinopyroxene-liquid equilibria using whole-rock geochemical and mineral chemical compositions help to distinguish the two situations. It is known, thus, that whereas the picrites and picritic basalts of the Western Ghats are normal evolved basalts enriched in cumulus olivine and clinopyroxene (Beane and Hooper, 1988; Sheth, 2005), those of the Saurashtra peninsula and Pavagadh, and some encountered in the Narmada region, represent near-primitive liquid compositions (West, 1958; Krishnamurthy and Cox, 1977; Melluso et al., 1995, 2006; Peng and Mahoney, 1995; Krishnamurthy et al., 2000). Melluso et al. (2006) report that the Sr–Nd–Pb isotopic compositions of the Pavagadh picrites are very similar to those of picritic basalts in Saurashtra. They modeled the incompatible element patterns of these estimated primitive liquids using a primitive mantle source and a non-fractional melting model. They assumed that melting of this primitive mantle source started in the garnet facies, and the melts of both garnet and spinel facies mixed variably to form the calculated melts. The Pavagadh picrites, with high  $\text{TiO}_2$ , appear to contain 23–42% of the total melt from garnet lherzolite, and Melluso et al. (2006) estimate the total percentage of partial melting to be between 4.8% and 6.2% for these rocks.

## 6.2. Closed-system fractional crystallization

Fig. 5 shows the chemical variation in some of the important elements with MgO. The mafic lavas have a significant range of variation, with MgO varying from 15 to 4 wt%. Correspondingly,  $\text{Al}_2\text{O}_3$  increases from 11 to 17.5 wt%,  $\text{SiO}_2$  from 44 to 51 wt%, and  $\text{TiO}_2$  increases up to 3.5 wt%. Fig. 6 shows the chemical variation in the sequence against stratigraphic height. High concentrations of Ba and other elements are encountered in the evolved lavas.

Major element mass balance calculations (with the program XLFRAC, Stormer and Nicholls, 1978) allow the transition from magmas such as D81 and D97 to evolved basalts through moderate (42–67%) fractionation of assemblages dominated by clinopyroxene and olivine, with lower amounts of plagioclase and oxides (Table 5). The transition from evolved basalts to rhyolites was modeled through fractionation of assemblages dominated by relatively sodic plagioclase (roughly half of the crystal extract), with a significant contribution of clinopyroxene and oxides (Table 5). Apatite and Fe-rich olivine are minor. As a result, the evolved rhyolites can be produced after 84–89% total fractionation of a solid with the composition of an olivine gabbro.

The Sr-isotopic compositions of basalts and rhyolites (Table 4), however, make closed-system fractional crystallization untenable. Open-system processes must be invoked in a small but significant degree, besides fractional crystallization, to explain the evolved rocks.

## 6.3. Assimilation and fractional crystallization (AFC)

The process of concurrent assimilation and fractional crystallization (AFC, DePaolo, 1981) is more realistic than simple fractional crystallization or bulk mixing, as the heat required for assimilation of contaminant can be supplied by the latent heat of crystallization of the magma (Bowen, 1928). Effects of AFC are often significantly different from those of bulk mixing. In the latter, the concentration of an element in the magma changes in the direction of that in the contaminant, but not necessarily so in AFC, where the change in concentration of residual magma depends not only on the concentration of that element in the contaminant and the degree of contamination, but also the degree of fractional crystallization and the concentration of the element in the fractionation assemblage.

AFC modeling was performed for the Pavagadh basalts and rhyolite in terms of Sr concentrations and  $^{87}\text{Sr}/^{86}\text{Sr}$  ratios (Fig. 7), using two distinct crustal contaminants

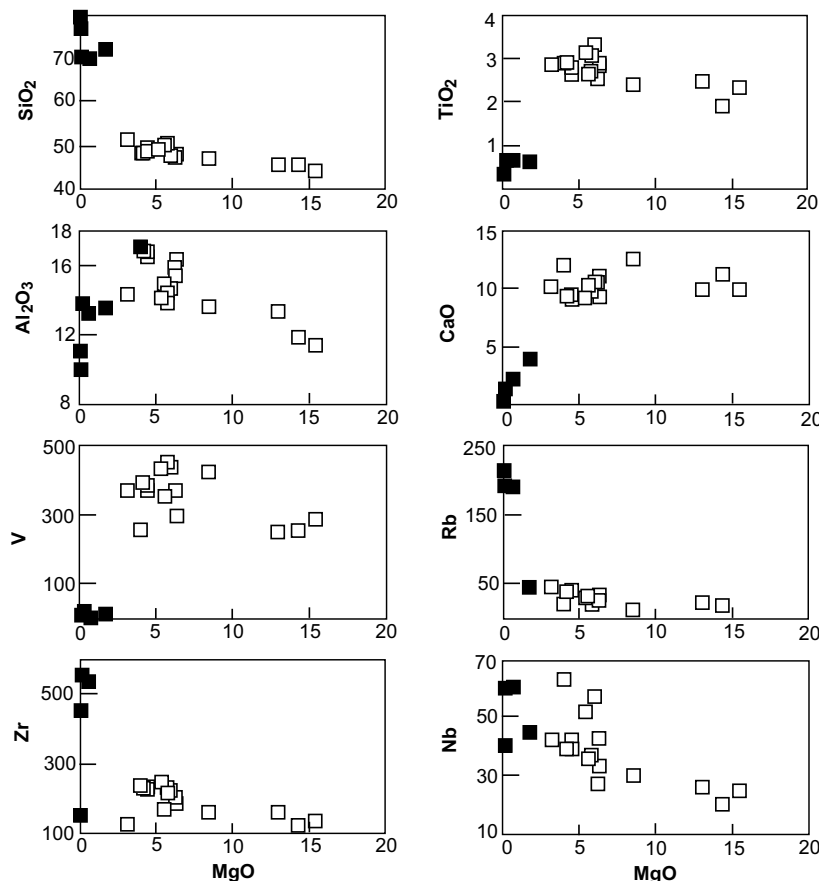


Fig. 5. Major and trace element variations with MgO in the Pavagadh suite of rocks. Oxides are in wt%, elements in ppm.

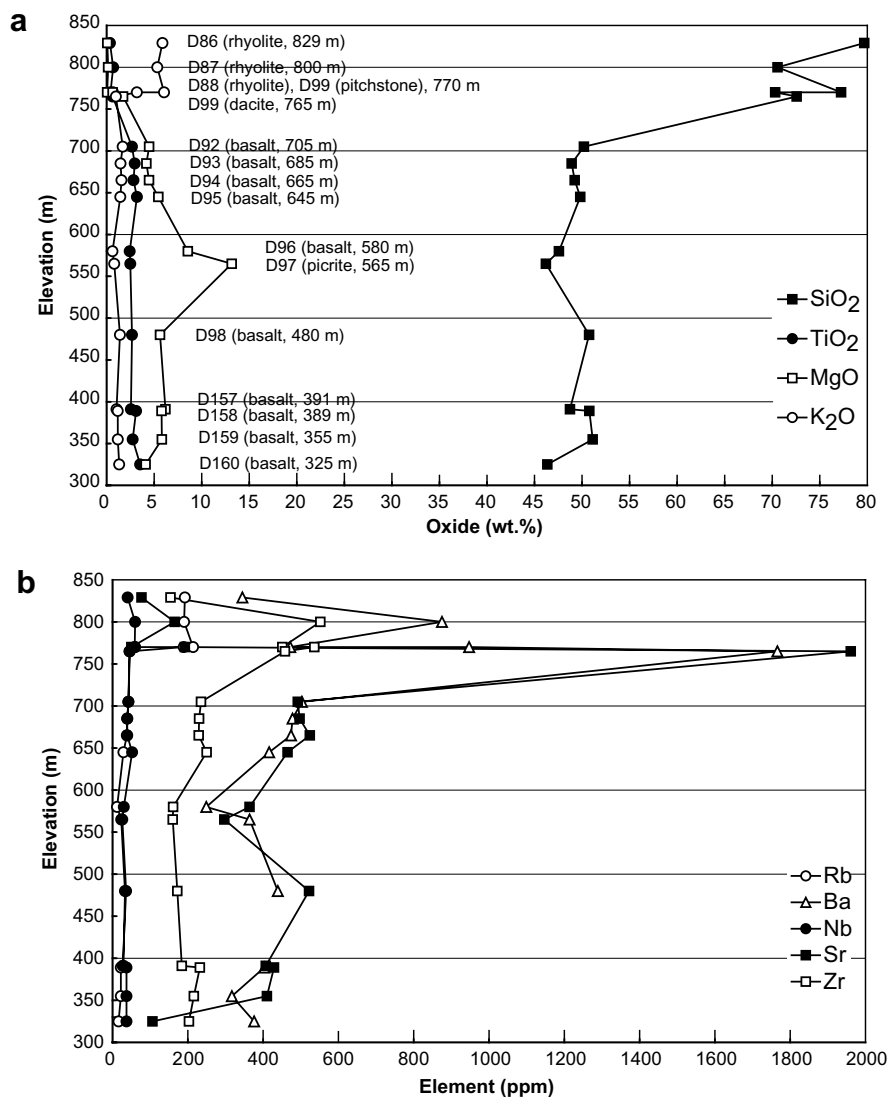


Fig. 6. Chemical variation with elevation on Mount Pavagadh.

and a single starting picritic magma (D97, with  $Sr = 297$  ppm,  $^{87}Sr/^{86}Sr = 0.70450$ ) for each. It was found that a two-stage AFC process with either contaminant explains the data quite well.

### 6.3.1. AFC Model 1

In this model (Fig. 7a) the crustal end member is a southern Indian granite (Peucat et al., 1989) with  $Sr = 160$  ppm and  $^{87}Sr/^{86}Sr = 0.7258$ . The generation of the final evolved liquid (rhyolite D89, with  $Sr = 192$  ppm and  $^{87}Sr/^{86}Sr = 0.70826$ ) was achieved in two stages. During the first stage, the basalt magma D97 was contaminated by the granite and simultaneously underwent fractional crystallization (bulk partition coefficient for Sr,  $D_{Sr} = 0.51$ ) to produce the evolved basalt magma D79, with  $Sr = 510$  ppm and  $^{87}Sr/^{86}Sr = 0.70626$ . The value of  $r$  (the ratio of the rate of assimilation to the rate of fractional crystallization, DePaolo, 1981) is 0.15, and D79 represents a residual liquid ( $F = 0.321$ ) left after 67.9% crystallization of the starting D97 magma. This value of

$F$  was determined from DePaolo's (1981) equation for isotopic ratio, using the value of the parameter  $z = (r + D - 1)/(r - 1)$  (see Sheth and Ray, 2002).

During the second stage, D79 was contaminated by the same granite and simultaneously fractionated ( $D_{Sr} = 1.8$ ) to produce the rhyolite D89. The value of  $r$  is 0.18, and D89 represents a residual liquid ( $F = 0.403$ ) left after ~59.7% fractional crystallization of the D79 magma. The figure also shows that the rhyolite D87 ( $Sr = 165$ ,  $^{87}Sr/^{86}Sr = 0.70639$ ) can be derived by nearly pure fractional crystallization of the basalt D79.

### 6.3.2. AFC Model 2

In this model (Fig. 7b) the crustal end member is a western Indian granite with  $Sr = 145$  ppm and  $^{87}Sr/^{86}Sr = 0.7690$  (Gopalan et al., 1979). This granite outcrops at Godhra (Fig. 1), only ~50 km NNE of Pavagadh. The generation of the final evolved liquid (rhyolite D89, with  $Sr = 192$  ppm and  $^{87}Sr/^{86}Sr = 0.70826$ ) was achieved in two stages. During the first stage, the basalt magma

Table 5  
Mass balance calculations for closed-system fractional crystallization

From	to	ol	cpx	Cr-Al-sp	pl		$\sum R^2$	% Removed solid	
D81	D156	36.8	40.3	4.3	18.5	100.0	0.15	50.7	
D81	D79	32.7	45.1	4.8	17.4	100.0	0.31	52.9	
D81	D80	33.2	33.8	5.6	27.4	100.0	0.33	67.1	
D81	D84	37.7	35.4	2.8	24.1	100.0	0.15	53.0	
D97	D79	37.8	33.0	9.2	20.1	100.0	0.12	42.1	
		ol	cpx	Sp	pl				
D97	D80	38.1	18.2	5.5	38.1	100.0	0.25	62.8	
D97	SH92	33.8	22.2	5.5	38.5	100.0	0.32	63.7	
		Fe-ol	cpx	sp	Na-pl	ap			
D80	D89	2.6	36.1	11.9	48.0	1.4	100.0	0.63	70.3
D84	D89	9.7	28.2	11.3	50.0	0.9	100.0	0.53	86.2
From	to	ol	cpx	sp	pl	ap		% Removed solid	
D81	D80	22.3	22.7	3.7	18.4			67.1	
D80	D89	1.8	25.4	8.3	33.7	1.0		70.3	
D81	D89	22.7 <sup>a</sup>	28.6	5.7	26.2	0.2		83.4	16.6 Residual liquid
D81	D84	20.0	18.8	1.5	12.8			53.0	
D84	D89	8.3	24.3	9.7	43.1	0.8		86.2	
D81	D89	23.4 <sup>b</sup>	28.6	5.4	30.2	0.3		87.9	12.1 Residual liquid
D97	D80	24.0	11.5	3.5	24.0			62.8	
D80	D89	2.6	36.1	11.9	48.0	1.4		100.0	
D97	D89	25.0 <sup>c</sup>	24.9	7.9	41.8	0.5		100.0	

<sup>a</sup> 22.7 = 22.3 + 1.8 (1–0.671)\* 0.703.

<sup>b</sup> 23.4 = 20.0 + 8.3 (1–0.53)\* 0.862.

<sup>c</sup> 25.0 = 24.0 + 2.6 (1–0.628)\* 1.00.

D97 was contaminated by the granite and simultaneously underwent fractional crystallization (bulk partition coefficient for Sr,  $D_{Sr} = 0.51$ ) to produce the evolved basalt magma D79, with Sr = 510 ppm and  $^{87}\text{Sr}/^{86}\text{Sr} = 0.70626$ . The value of  $r$  is 0.06, and D79 represents a residual liquid ( $F = 0.326$ ) left after 67.4% crystallization of the starting D97 magma. During the second stage, D79 was contaminated by the same granite and simultaneously fractionated ( $D_{Sr} = 1.8$ ) to produce the rhyolite D89. The value of  $r$  is only 0.055, and D89 represents a residual liquid ( $F = 0.328$ ) left after 67.2% fractional crystallization of the D79 magma. Note that bulk mixing of a D97 magma with either the south Indian or the western Indian granite contaminant cannot explain the compositions of the lavas (Fig. 7a and b).

Alexander (1981) reported a high  $^{87}\text{Sr}/^{86}\text{Sr}$  ratio of 0.7111 in the Pavagadh rhyolite and correctly argued for the involvement of the continental crust, but did not mention from where the sample came (the summit lava, or the rhyolite blocks that lie scattered on the lower slopes of the mountain, probably a separate eruption). No attempt is therefore made here to explain his isotopic value.

#### 6.4. Degree of crustal contamination

DePaolo (1981) defined the parameter  $r$  as the ratio of the rate of assimilation (mass assimilated per unit time) to the rate of fractional crystallization (mass fractionated per unit time). His AFC modeling and equations do not yield a value for the degree or amount of contamination,

however. Sheth and Ray (2002) extended the scope of the AFC modeling by deriving a mathematical expression for the degree of contamination ( $C$ ), which is:  $C\% = r(1-F)/(1-r)$ . They meant, by degree of contamination at any given instant, the ratio of the mass of total assimilated material to the initial mass of the magma as at that instant. Using this equation, the degree of crustal contamination suffered by the residual liquids D79 and D89 was calculated, for either contaminant. All that is required is values of  $r$  and  $F$  represented by a particular residual liquid. With the southern Indian granite as the contaminant (Fig. 7a), the equation of Sheth and Ray (2002) yields a contamination value of 11.98% in the production of the basalt D79 from the picrite D97, and a contamination of 13.10% in the production of the rhyolite D89 from the basalt D79. On the other hand, with the western Indian granite as the contaminant (Fig. 7b), the equation yields a contamination value of 4.30% in the production of the basalt D79 from the picrite D97, and a contamination of 3.91% in the production of the rhyolite D89 from the basalt D79. The percentage contamination implied or required by the residual liquids D79, or D89, with the western Indian granite as a contaminant is significantly less (~4%) than that with the south Indian granite (12–13%). This is clearly because of the much higher  $^{87}\text{Sr}/^{86}\text{Sr}$  ratio of the western (0.7690) than the southern (0.7258) Indian granite. Sr concentration also obviously is a factor, but not in this specific case as both granites differ by only ~10% in their Sr concentration (145 vs. 160 ppm).

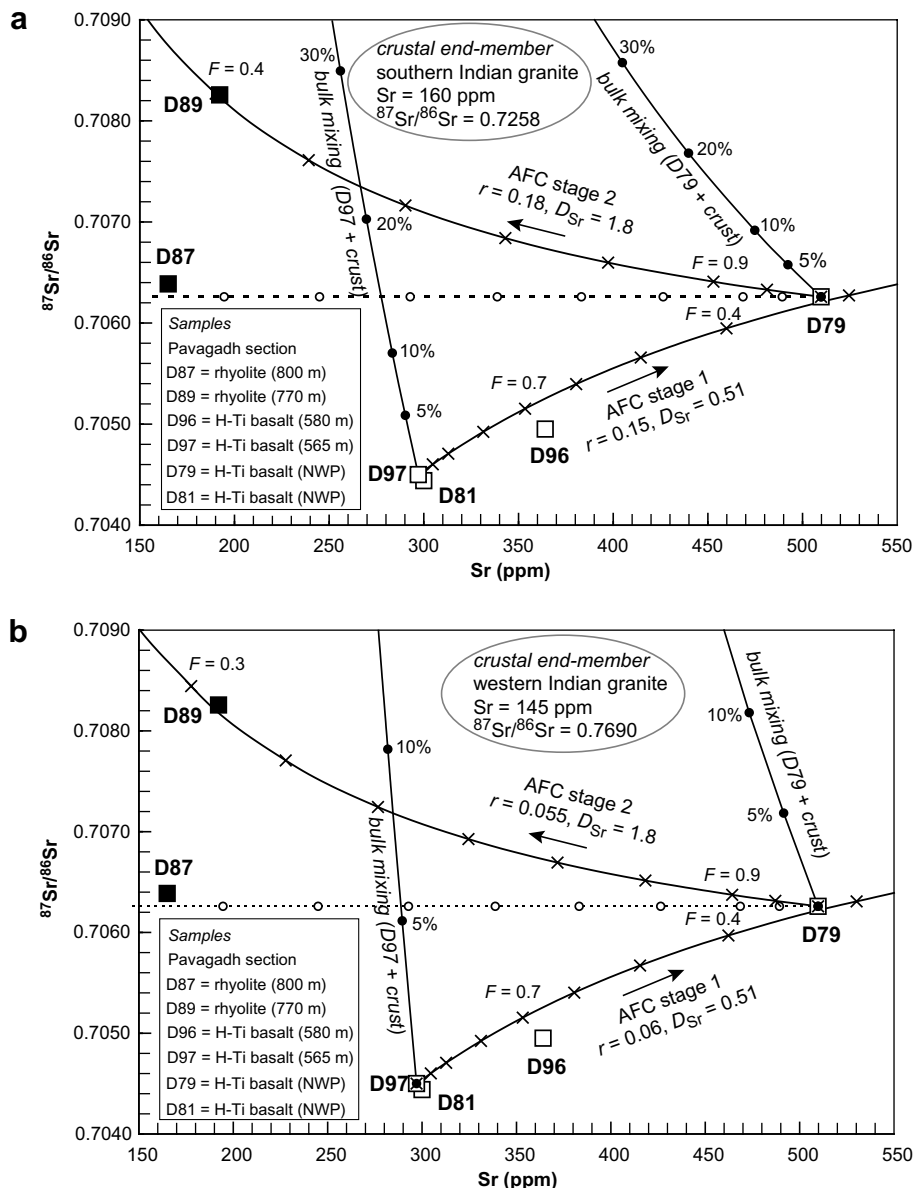


Fig. 7. AFC modeling for the Pavagadh basalts and rhyolites, using (a) southern Indian granite as a contaminant and (b) western Indian granite as a contaminant. The  $D_{Sr}$  values of 0.51 and 1.8 for AFC stage 1 and stage 2, respectively, are based on the following  $K_d$  values for Sr (Arth, 1976; Watson and Green, 1981; Rollinson, 1993): Stage 1 (olivine, 0.014; clinopyroxene, 0.06; plagioclase, 2.1), stage 2 (olivine, 0.014; clinopyroxene, 0.516; sodic plagioclase, 3.3; apatite, 1.3).

## 7. Geochemical comparisons and stratigraphic correlations of the Pavagadh lavas

Geochemical comparisons and geochemical stratigraphic correlations across the Deccan province, that are now routinely performed (Peng et al., 1998; Mahoney et al., 2000; Sheth et al., 2004a; Bondre et al., 2006) have combined three or all of the following four approaches: (i) binary plots of incompatible element concentrations and concentration ratios, (ii) comparison of the primitive-mantle-normalized multielement patterns of the samples with patterns of the southwestern lavas, (iii) comparison of Sr–Nd–Pb isotopic ratios, and (iv) discriminant function analysis employing major elements and several commonly

analyzed trace elements. The same approach is followed here.

### 7.1. Binary discrimination diagrams

A useful tabulated summary of key element (Sr, Ba), element ratio (Ba/Y, Zr/Nb), and Sr-isotopic ranges of various formations making up the Western Ghats stratigraphy can be found in Mitchell and Widdowson (1991). Fig. 8 compares element concentrations and concentration ratios in the Pavagadh basalts and picrites to those of the Western Ghats formations (624 samples, Beane, 1988), the Bhuj basanites (Karmalkar et al., 2005), the high-Nb-Ba Toranmal lavas (Mahoney et al., 2000), as

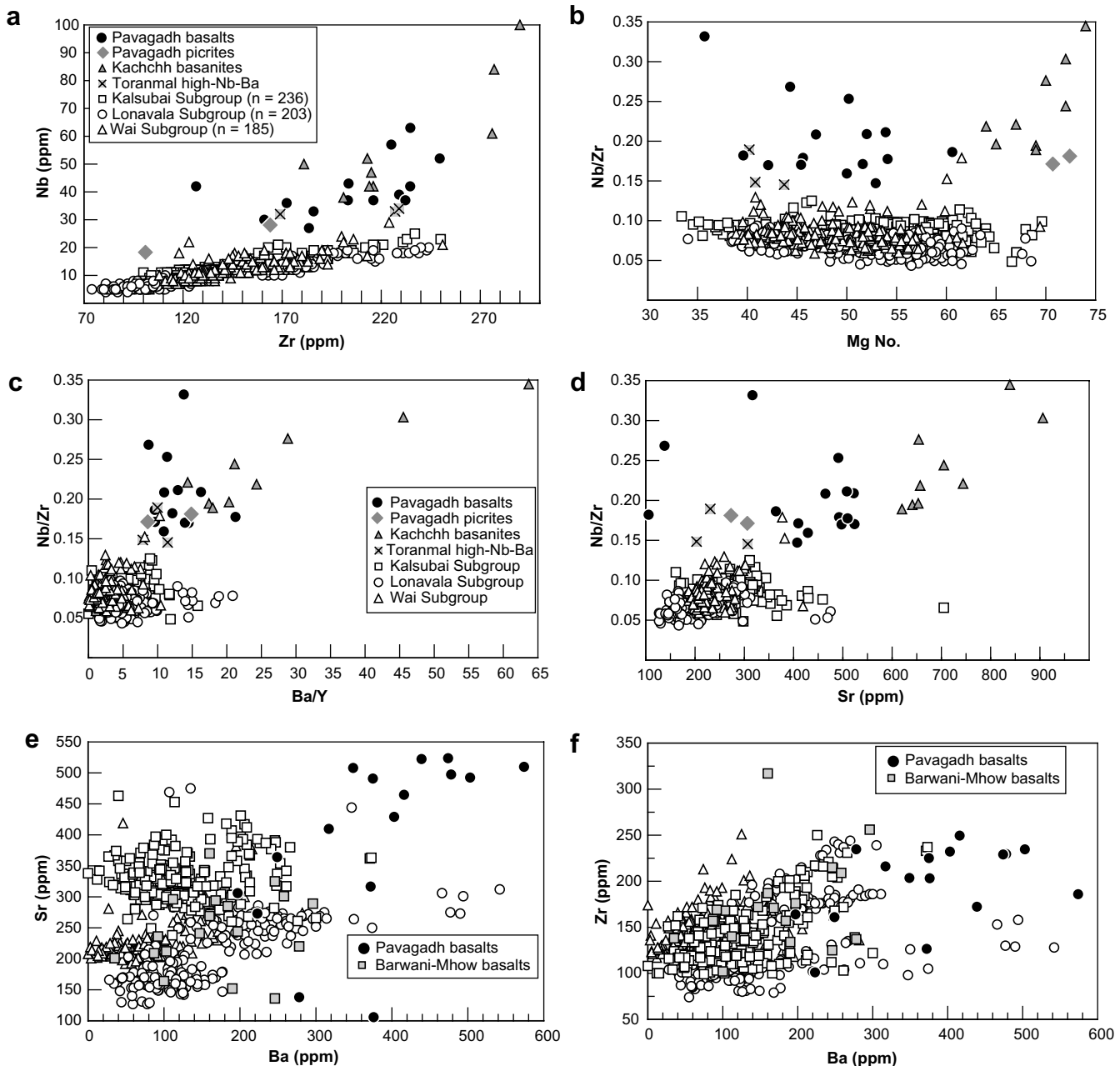


Fig. 8. Binary geochemical variation diagrams of incompatible elements and element ratios for the Pavagadh mafic rocks (filled circles are basalts, filled diamonds are picrites). Data for the Western Ghats formations (624 samples, [Beane, 1988](#)), the Kachchh basanites ([Karmalkar et al., 2005](#)), the high-Nb-Ba lavas at Toranmal ([Mahoney et al., 2000](#)), and the Barwani–Mhow basalts ([Sreenivasa Rao et al., 1985](#)) are shown for comparison. Throughout the six panels, open squares are Kalsubai Subgroup lavas, open circles are Lonavala Subgroup lavas, and open triangles are Wai Subgroup lavas.

well as the basalts exposed between Barwani and Mhow ([Sreenivasa Rao et al., 1985](#)). The Pavagadh rocks are clearly separated from the Western Ghats formations on a plot of Nb vs. Zr (Fig. 8a). The Pavagadh basalts have Zr values comparable to or slightly higher than that of many Western Ghats basalts, but their Nb values are considerably higher, like those of a few flows at Toranmal section for example. [Mahoney et al. \(2000\)](#) could not correlate these Toranmal lavas to the Western Ghats lavas.

The Nb/Zr ratio changes little even during extreme sub-aerial alteration, due to both elements having approximately similar mobilities, and is therefore one of the most useful in petrogenetic interpretations and geochemical comparisons of altered Deccan basalts, and in fact even the laterites derived from them (e.g., [Mitchell and Widdowson, 1991](#); [Widdowson and Cox, 1996](#)). The Mahabaleshwar Formation basalts have the highest Nb/Zr ratios among the Western Ghats lavas, but the Pavagadh basalts have still higher values. Notably, the Pavagadh and

Western Ghats basalt lavas have the same range of Mg Number (Fig. 8b), though their near-total separation in terms of Nb/Zr is evident in Fig. 8b, the Pavagadh samples having systematically higher values ( $>0.15$ ) than the Western Ghats lavas (mostly 0.05–0.10). Fig. 8c is a plot of Nb/Zr vs. Ba/Y. Y is also resistant to alteration, and Sr and Ba are much less mobile than K or Rb; however, with advanced alteration, Si, Ca, P, Ni, Sr, Y, Ba, and the REE are all modified relative to elements such as Al, Nb, Zr, Fe, Cr, and Ti (e.g., Widdowson and Cox, 1996; Mahoney et al., 2000). Both Nb/Zr and Ba/Y ratios are also relatively insensitive to fractional crystallization of minerals common in basaltic liquids. The Pavagadh samples also have Ba/Y ratios higher than the Western Ghats lavas, except a few Khandala Formation lavas. The same clear separation of the Pavagadh basalts from almost all the Western Ghats lavas persists on a plot of Sr vs. Nb/Zr (Fig. 8d). Thus, the Pavagadh basalts, though mostly sub-alkalic and as evolved as the Western Ghats lavas, have unusually high Nb concentrations and Nb/Zr ratios, and these characteristics cannot be explained by variable amounts of fractional crystallization or subaerial alteration. Nb is a strongly incompatible element, with Zr only slightly less so. Based on these key element and element ratio plots, none of the Pavagadh section basalts can be grouped with any of the Western Ghats formations including the uppermost Panhala Formation. Despite having the same (normal) magnetic polarity as the upper Pavagadh basalts, all Panhala lavas have Sr  $< 200$  ppm, Ba  $< 90$  ppm, and TiO<sub>2</sub>  $< 2.3$  wt% (Lightfoot and Hawkesworth, 1988; Lightfoot et al., 1990; Mitchell and Widdowson, 1991). Most Pavagadh basalts have Sr and Ba values of 400–500 ppm, and TiO<sub>2</sub> values well over 2.5 wt% (Tables 2 and 3).

A thorough geochemical comparison of the Pavagadh basalts to the basalt lavas forming sizeable sections between Barwani and Mhow (Fig. 1) cannot be attempted, because published geochemical data for these latter are limited to the major oxides and Ba, Sr and Zr contents (Sreenivasa Rao et al., 1985); no isotopic data exist. (No direct correlations of these sections to the Western Ghats have been possible either.) Fig. 8e and f compare the Ba–Sr–Zr contents of the Pavagadh, the Satpura–Narmada, and the Western Ghats lavas, and show that the Pavagadh basalts cannot be correlated with any of these basalts in terms of these three elements combined.

### 7.2. Normalized multielement patterns

Fig. 9a shows the primitive-mantle-normalized multielement patterns for some of the Pavagadh lavas. The Pavagadh picrites D81 and D97 have patterns closely similar to the central Saurashtra picrite D44 analyzed by Melluso et al. (1995). The patterns resemble those of ocean island basalts, and the Mahabaleshwar Formation pattern is broadly similar. The basanites of Kachchh (Karmalkar et al., 2005) have patterns that are very similar in shape,

though displaced at higher incompatible element contents, thus suggesting similarity in the mantle source signature.

Fig. 9b shows the primitive-mantle-normalized multielement patterns of two of the Pavagadh basalts. The patterns of the basalts D158 and D79 are steeply sloping to the right, and are therefore easily distinguished from those of the Ambenali and Mahabaleshwar Formations. The basalt patterns are similar to the Khandala Formation basalt patterns, and yet there are significant differences, especially in Ba and the heavier elements, so that the patterns cross. It is safe to conclude on the basis of multielement patterns, that the Pavagadh basalts do not closely resemble any of the Western Ghats formations or members or individual lava flows.

### 7.3. Discriminant function analysis

Discriminant function analysis would not be helpful in the present case, given the very clear separations between the Pavagadh and the Western Ghats lavas in many elements, element ratios, and multielement patterns. The analysis was nevertheless executed twice (the first run using the major oxides SiO<sub>2</sub>, Al<sub>2</sub>O<sub>3</sub>, Fe<sub>2</sub>O<sub>3</sub>, FeO, CaO, MgO, K<sub>2</sub>O, and P<sub>2</sub>O<sub>5</sub>, and the second using the trace elements Ni, V, Ba, Rb, Sr, Zr, Y, and Nb), following exactly the methodology of recent workers who have found it useful or extremely useful (Peng et al., 1998; Mahoney et al., 2000; Sheth et al., 2004a; Bondre et al., 2006). As expected, both runs yielded zero probability of any of the Pavagadh lavas being grouped with any of the Western Ghats formations. The tabulated results are available from the authors.

## 8. Discussion

It is evident that the Pavagadh section is chemically and genetically unrelated to the Western Ghats lava pile, and to sections in the north and northeast of the province (where thick lava piles closely resemble the Western Ghats lava pile, in the elements and also Nd–Sr isotopes and sometimes Pb isotopes, Peng et al., 1998). In no way does this reduce the value of chemostratigraphy or magnetic polarity stratigraphy as correlation tools, of course. Rather, it appears that separate but possibly coeval eruptive centers, with their own distinctive chemistries, developed in different areas.

A few basalts in the northwest have characteristics such as high Nb concentrations resembling the Pavagadh basalts (e.g., the Anjar basalts, with Nb from 19 to 64 ppm, Shukla et al., 2001). The Navagam basalts exposed on the Narmada River (Mahoney et al., 1985; Melluso et al., 1995) are also notable in having such uniformly high Nb concentrations. In contrast, only a few flows of the Toranmal section (Mahoney et al., 2000), Rajpipla (Krishnamurthy and Cox, 1980; Mahoney et al., 1985; Melluso et al., 1995) and Mhow (Peng et al., 1998) have such high ( $\geq 30$  ppm) Nb values. It is noteworthy here that the few high-Nb Toranmal flows also could not be correlated with any of

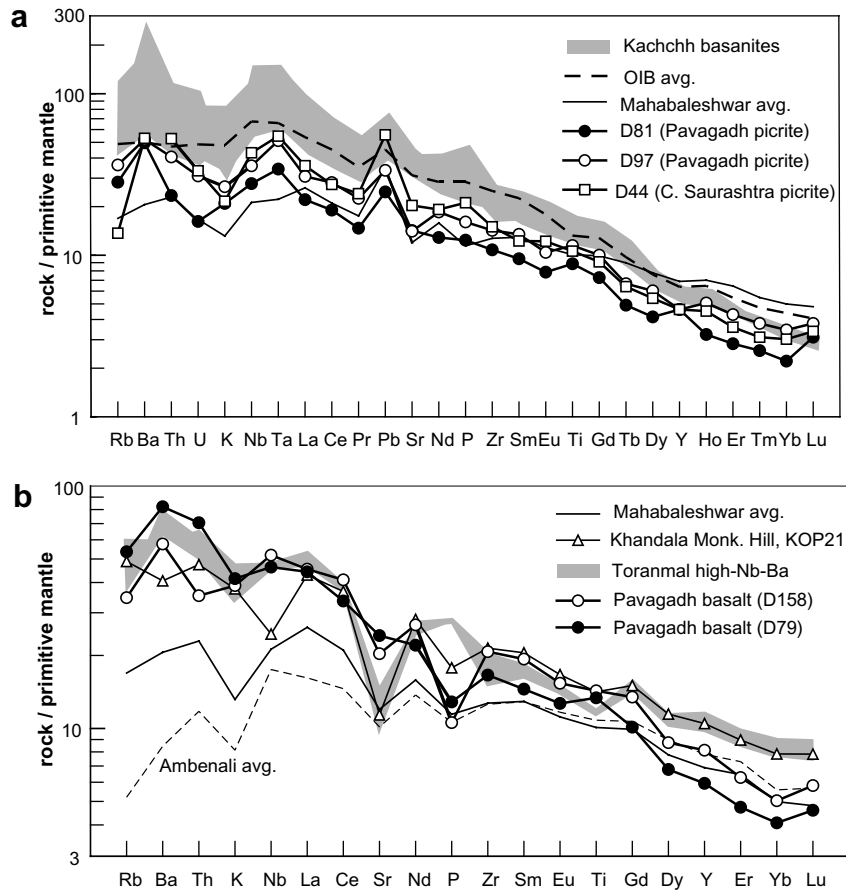


Fig. 9. (a) Primitive-mantle-normalized multi-element patterns for Pavagadh picrites, compared to those of ocean island basalts (Sun and McDonough, 1989), Kachchh basanites (Karmalkar et al., 2005), and the central Saurashtra picrite (D44, Melluso et al., 1995). Normalizing values are from Sun and McDonough (1989). (b) Patterns for two of the Pavagadh basalts, compared to those of the high-Nb–Ba flows of Toranmal section (Mahoney et al., 2000) and some Deccan formation averages (courtesy J.J. Mahoney).

the Western Ghats formations or lavas on the basis of combined multi-element and statistical methods (Mahoney et al., 2000). Notably, published Nb values for basalts of the Western Ghats are all <30 ppm, the highest being known in the Mahabaleshwar Formation (Kolhapur Unit, Lightfoot et al., 1990). By comparison, basanites of Kachchh, northwest Deccan, contain 38–100 ppm Nb and 418–1783 ppm Ba; these are, of course, alkalic and highly silica-undersaturated rocks ( $\text{SiO}_2 = 40.39\text{--}43.69\%$ ; Fig. 2). The picrites and the basanites could be the products of somewhat different degrees of partial melting of similar “enriched” mantle sources, located below western India in late Cretaceous time (Melluso et al., 1995).

As also seen, the available geochemical and Sr-isotopic data for the Pavagadh sequence are consistent with a two-stage AFC process involving a picritic starting magma and either of two granite contaminants. During AFC, residual liquids become progressively more contaminated as they evolve by fractional crystallization, and such magma suites show a negative correlation between indices of crustal contamination (such as  $^{87}\text{Sr}/^{86}\text{Sr}$ ) and of fractional crystallization (e.g., Mg Number). On the other hand, the dramatically different mechanism of tempera-

ture-controlled assimilation (more primitive magmas experiencing systematically greater amounts of contamination due to being hotter) has been well known from the Western Ghats, particularly the Bushe and Poladpur Formation lavas (e.g., Devey and Cox, 1987; Lightfoot and Hawkesworth, 1988; Mahoney, 1988). This is another line of evidence suggesting that the Pavagadh sequence should be viewed outside of the Western Ghats stratigraphic framework.

No Ar–Ar age data exist for the Pavagadh rocks, and the only absolute ages in the literature are K–Ar ages of  $\sim 66$  Ma obtained by Kaneoka and Haramura (1973) on a basalt and ankaramite. The authors did not specify their locations or sampling heights, but noted on the basis of their hydrated nature of the samples ( $\text{H}_2\text{O}^+ \sim 2.2$  wt%) that the K–Ar ages should be considered minimum ages. The Pavagadh lavas then probably belong to the early phases of Deccan Trap volcanicity. Even if future Ar–Ar age data on Pavagadh rocks fall within the age bracket of eruption of the Western Ghats lavas (itself the matter of considerable debate, see e.g., Kaneoka, 1980; Courtillot et al., 1986; Wensink, 1987; Hofmann et al., 2000; Pande, 2002), the differences in geochemistry and magnetic polar-

ity between the Pavagadh and the Western Ghats lavas convincingly rule out any relationship between the two. The normally magnetized Pavagadh sequence is probably older than the Jawhar Formation, the oldest in the Western Ghats stratigraphy (Table 1). Feeder dykes for the Pavagadh sequence should be sought, and these may outcrop in the Rajpipla-Navagam region.

The trace element ratios, and rare earth element patterns show at least three different magma types in the area between Pavagadh, Saurashtra to the northwest, and the central Deccan: (1) low-Zr/Y basalts ( $Zr/Y=2.9-5.3$ , average  $3.7 \pm 2.0$ ,  $2\sigma$  error) have slightly fractionated light-REE patterns, with flat heavy REE patterns, and abundances lower than 60X chondrite; (2) moderate-Zr/Y basalts ( $Zr/Y=3.9-5.7$ , average  $4.7 \pm 1.2$ ,  $2\sigma$ ), have moderately fractionated REE patterns, with abundances lower than 100X chondrite, and (3) high-Zr/Y basalts ( $Zr/Y=5.9-8.2$ , average  $6.5 \pm 1.6$ ,  $2\sigma$ ), with highly fractionated REE patterns. The mantle normalized diagrams also show that the rocks with flat heavy REE patterns have negative Nb peaks, whereas the high-Zr/Y basalts have peaks at Nb. The Pavagadh basalts have some of the most “enriched” trace element compositions among the various basalt types of the Deccan province.

The relatively high initial  $^{87}\text{Sr}/^{86}\text{Sr}$  ratios (0.7064 and 0.7083) of Pavagadh rhyolites indicate open-system processes, with a small chemical contribution from the continental crust, and allow an evaluation of the role of crustal melting in the genesis of the silicic rocks of the Deccan province as a whole. Whereas Lightfoot et al. (1987) argued that the rhyolites and trachytes of Bombay (Fig. 1), on the west coast, were products of fractional crystallization of basaltic magmas or partial melting of deep-seated basalt piles, Sheth and Ray (2002) developed an assimilation–fractional crystallization (AFC) model for these rocks in terms of their Sr-concentrations and Sr-isotopic compositions, using the same western Indian granite contaminant as used here. Chatterjee and Bhattacharji (2001, 2004) have also argued for significant crustal involvement, based on geochemical criteria, in the genesis of the silicic rocks of eastern and southern Saurashtra. Overall, therefore, the genesis of silicic rocks in the Deccan, the Pavagadh rhyolites included, appears to have involved at least some anatexis of the basement crust, and this may be a necessary consequence of the heat conducted and advected into the crust by large volumes of mafic magma ponded at the base of the crust and periodically passing through it (Cox, 1980).

## 9. Conclusions

Much of the ~550-m thick exposed section on Mount Pavagadh, Deccan Traps, is made up of subalkalic basalts rich in incompatible elements (especially Nb and Ba), and Sr. Rhyolite-dacite flows and pyroclastic rocks also occur at the top of the sequence. The  $^{87}\text{Sr}/^{86}\text{Sr}$  ratios and chemical characteristics of the Pavagadh rhyolites suggest a

small but significant involvement of the granitic basement crust in their genesis. An assimilation–fractional crystallization (AFC) model involving the picrite lava and granitic crustal contaminants explains the geochemical and Sr-isotopic variation in the basalts and the rhyolites quite well. Systematic comparison of the lavas to the well-established lava stratigraphy of the Western Ghats, several hundred kilometers to the south, reveals that no chemical–genetic relationship is possible between the two. A few sections close to Pavagadh, such as Toranmal and Navagam, show a few to many flows with similar chemical characteristics, but no straightforward correlations are achievable between the Pavagadh sequence and the sequences in the Toranmal–Navagam–Barwani–Mhow region, especially if their magnetic polarities are also considered. The new geochemical data on the compositionally varied Pavagadh volcanic suite are significant in understanding similarly diverse lava sequences elsewhere, the evolution of silicic lavas in flood basalt provinces, as well as the regional stratigraphy of the Deccan Traps, where large individual areas seem to have developed magmatic systems and lava piles with their own distinctive chemical and/or isotopic signatures.

## Acknowledgments

Surendra Pal Verma kindly provided the SINCLAS program, and John Mahoney, unpublished geochemical data on various Deccan formations. Constructive, in-depth reviews by Ninad Bondre and Mike Widdowson and the editorial input from Bor-ming Jahn are gratefully acknowledged.

## References

- Alexander, P.O., 1981. The Pavagarh rhyolite. *J. Geol. Soc. Ind.* 21, 453–457.
- Arth, J.G., 1976. Behaviour of trace elements during magmatic processes – a summary of theoretical models and their applications. *J. Res. U.S. Geol. Surv.* 4, 41–47.
- Beane, J.E., 1988. Flow Stratigraphy, Chemical Variation and Petrogenesis of Deccan Flood Basalts from the Western Ghats, India. Ph.D. Dissertation, Washington State University, USA.
- Beane, J.E., Hooper, P.R., 1988. A note on the picrite basalts of the Western Ghats, Deccan Traps. In: Subbarao, K.V. (Ed.), *Deccan Flood Basalts*. *Geol. Soc. Ind. Mem.* 10, pp. 117–134.
- Beane, J.E., Turner, C.A., Hooper, P.R., Subbarao, K.V., Walsh, J.N., 1986. Stratigraphy, composition and form of the Deccan basalts, Western Ghats, India. *Bull. Volcanol.* 48, 61–83.
- Bellieni, G., Brotzu, P., Comin-Chiaromonti, P., Ernesto, M., Melfi, A., Pacca, I.G., Piccirillo, E.M., 1984. Flood basalt to rhyolite suites in the southern Parana plateau (Brazil): Palaeomagnetism, petrogenesis, and geodynamic implications. *J. Petrol.* 25, 579–618.
- Betton, P.J., 1979. Isotopic evidence for crustal contamination in the Karoo rhyolites of Swaziland. *Earth Planet. Sci. Lett.* 45, 263–274.
- Bilgrami, S.Z., 1999. A geological map of the eastern part of the Deccan Traps (Bidar-Nagpur). In: Subbarao, K.V. (Ed.), *Deccan Volcanic Province*. *Geol. Soc. Ind. Mem.* 43(1), 219–232.
- Bondre, N.R., Hart, W.K., Sheth, H.C., 2006. Geology and geochemistry of the Sangamner mafic dyke swarm, western Deccan volcanic province, India: implications for regional stratigraphy. *J. Geol.* 114, 155–170.

- Bowen, N.L., 1928. The Evolution of the Igneous Rocks. Princeton University Press, Princeton, New Jersey, pp. 334.
- Chatterjee, A.C., 1961. Petrology of the lavas of Pavagadh Hill, Gujarat. *J. Geol. Soc. Ind.* 2, 61–77.
- Chatterjee, N., Bhattacharji, S., 2001. Origin of the felsic and basaltic dykes and flows in the Rajula–Palitana–Sihor area of the Deccan Traps, Saurashtra, India: a geochemical and geochronological study. *Int. Geol. Rev.* 43, 1094–1116.
- Chatterjee, N., Bhattacharji, S., 2004. A preliminary geochemical study of zircons and monazites from Deccan felsic dykes, Rajula, Gujarat, India: implications for crustal melting. In: Sheth, H.C., Pande, K. (Eds.), *Magmatism in India through Time*. Proc. Ind. Acad. Sci. (Earth Planet. Sci.) vol. 113, pp. 533–542.
- Comin-Chiaromonti, P., Cundari, A., Piccirillo, E.M., Gomes, C.B., Castorina, F., Censi, P., De Min, A., Marzoli, A., Speziale, S., Velazquez, V.F., 1997. Potassic and sodic igneous rocks from eastern Paraguay: their origin from the lithospheric mantle and genetic relationships with the associated Parana flood tholeiites. *J. Petrol.* 38, 495–528.
- Courtillot, V., Besse, J., Vandamme, D., Montigny, R., Jaeger, J.-J., Cappetta, H., 1986. Deccan flood basalts at the Cretaceous/Tertiary boundary? *Earth Planet. Sci. Lett.* 80, 361–374.
- Cox, K.G., 1980. A model for flood basalt vulcanism. *J. Petrol.* 21, 629–650.
- Cox, K.G., Hawkesworth, C.J., 1985. Geochemical stratigraphy of the Deccan Traps at Mahabaleshwar, Western Ghats, India, with implications for open system magmatic processes. *J. Petrol.* 26, 355–377.
- DePaolo, D.J., 1981. Trace element and isotopic effects of combined wall rock assimilation and fractional crystallization. *Earth Planet. Sci. Lett.* 53, 189–202.
- Devey, C.W., Cox, K.G., 1987. Relationships between crustal contamination and crystallization in continental flood basalt magmas, with special reference to the Deccan Traps of the Western Ghats, India. *Earth Planet. Sci. Lett.* 84, 59–68.
- Dhandapani, R., Subbarao, K.V., 1992. Magnetostratigraphy of the Deccan lavas, south of the Narmada River. *Geol. Soc. Ind. Mem.* 24, 63–79.
- Eugster, H.P., Wones, D.R., 1962. Stability relations of the ferruginous biotite, annite. *J. Petrol.* 3, 82–125.
- Floyd, P.A., Winchester, J.A., 1978. Identification and discrimination of altered and metamorphosed volcanic rocks using immobile elements. *Chem. Geol.* 21, 291–306.
- Furuyama, K., Hari, K.R., Santosh, M., 2001. Crystallization history of primitive Deccan basalt from Pavagadh hill, Gujarat, western India. *Gond. Res.* 3, 427–436.
- Garland, F.E., Hawkesworth, C.J., Mantovani, M.S.M., 1995. Description and petrogenesis of the Parana rhyolites. *J. Petrol.* 36, 1193–1227.
- Gopalan, K., Trivedi, J.R., Merh, S.S., Patel, P.P., Patel, S.G., 1979. Rb–Sr age of Godhra and related granites, Gujarat, India. *Proc. Ind. Acad. Sci. (Earth Planet. Sci.)* 4, 7–17.
- Govindaraju, K., 1989. Compilation of working values and sample descriptions for 272 geostandards. *Geostand. Newslett.* 13, 1–113.
- Greenough, J.D., Hari, K.R., Chatterjee, A.C., Santosh, M., 1998. Mildly alkaline basalts from Pavagadh hill, India: Deccan flood basalts with an asthenospheric origin. *Mineral Petrol* 62, 223–245.
- Hari, K.R., Santosh, M., Chatterjee, A.C., 1991. Primary silicate-melt inclusions in olivine phenocrysts from the Pavagadh igneous suite, Gujarat. *J. Geol. Soc. Ind.* 37, 343–350.
- Hari, K.R., Santosh, M., Furuyama, K., 2000. Melt inclusions in pyroxene and plagioclase phenocrysts from Pavagarh igneous suite, Gujarat, India. *J. Geosci. Osaka City Univ.* 43, 135–148.
- Hofmann, C., Féraud, G., Courtillot, V., 2000.  $^{40}\text{Ar}/^{39}\text{Ar}$  dating of mineral separates and whole rocks from the Western Ghats lava pile: further constraints on duration and age of the Deccan Traps. *Earth Planet. Sci. Lett.* 180, 13–27.
- Irvine, T.N., Baragar, W.R.A., 1971. A guide to the chemical classification of the common rocks. *Can. J. Earth Sci.* 8, 523–548.
- Kaneoka, I., 1980.  $^{40}\text{Ar}/^{39}\text{Ar}$  dating on volcanic rocks of the Deccan Traps, India. *Earth Planet. Sci. Lett.* 46, 233–243.
- Kaneoka, I., Haramura, H., 1973. K/Ar ages of successive lava flows from the Deccan Traps, India. *Earth Planet. Sci. Lett.* 18, 229–236.
- Karmalkar, N.R., Rege, S., Griffin, W.L., O'Reilly, S.Y., 2005. Alkaline magmatism from Kutch, NW India: implications for plume–lithosphere interaction. *Lithos* 81, 101–119.
- Krishnamurthy, P., Cox, K.G., 1977. Picrite basalts and related lavas from the Deccan Traps of Western India. *Contrib. Mineral. Petrol.* 62, 53–75.
- Krishnamurthy, P., Cox, K.G., 1980. A potassium-rich alkalic suite from the Deccan Traps, Rajpipla, India. *Contrib. Mineral. Petrol.* 73, 179–189.
- Krishnamurthy, P., Gopalan, K., Macdougall, J.D., 2000. Olivine compositions in picrite basalts and the Deccan volcanic cycle. *J. Petrol.* 41, 1057–1069.
- Le Bas, M.J., 2000. IUGS reclassification of the high-Mg and picritic volcanic rocks. *J. Petrol.* 41, 1467–1470.
- Le Bas, M.J., LeMaitre, R.W., Streckeisen, A., Zanettin, P., 1986. A chemical classification of volcanic rocks based on the total alkali–silica diagram. *J. Petrol.* 27, 745–750.
- LePage, L.D., 2003. ILMAT: an Excel worksheet for ilmenite–magnetite geothermometry and geobarometry. *Comput. Geosci.* 29, 673–678.
- Lightfoot, P.C., Hawkesworth, C.J., Sethna, S.F., 1987. Petrogenesis of rhyolites and trachytes from the Deccan Trap: Sr, Nd, and Pb isotope and trace element evidence. *Contrib. Mineral. Petrol.* 95, 44–54.
- Lightfoot, P.C., Hawkesworth, C.J., 1988. Origin of Deccan Trap lavas: evidence from combined trace element and Sr-, Nd- and Pb-isotope studies. *Earth Planet. Sci. Lett.* 91, 89–104.
- Lightfoot, P.C., Hawkesworth, C.J., Devey, C.W., Rogers, N.W., van Calsteren, P.W.C., 1990. Source and differentiation of Deccan Trap lavas: implications of geochemical and mineral chemical variations. *J. Petrol.* 31, 1165–1200.
- Macdougall, J.D. (Ed.), 1988. *Continental Flood Basalts*. Kluwer Academic Publisher, Dordrecht, p. 341.
- Mahoney, J.J., 1988. Deccan Traps. In: Macdougall, J.D. (Ed.), *Continental Flood Basalts*. Kluwer Academic Publisher, Dordrecht, pp. 151–194.
- Mahoney, J.J., Coffin, M.F. (Eds.), 2007. *Large Igneous Provinces: continental, Oceanic, and Planetary Flood Volcanism*. Am. Geophys. Union Geophys. Monogr., vol. 100, pp. 438.
- Mahoney, J.J., Macdougall, J.D., Lugmair, G.W., Gopalan, K., Krishnamurthy, P., 1985. Origin of contemporaneous tholeiitic and K-rich alkalic lavas: a case study from the northern Deccan plateau, India. *Earth Planet. Sci. Lett.* 72, 39–53.
- Mahoney, J.J., Sheth, H.C., Chandrasekharam, D., Peng, Z.X., 2000. Geochemistry of flood basalts of the Toranmal section, northern Deccan Traps, India: implications for regional Deccan stratigraphy. *J. Petrol.* 41, 1099–1120.
- Marsh, J.S., Hooper, P.R., Rehacek, J., Duncan, R.A., Duncan, A.R., 1997. Stratigraphy and age of Karoo basalts of Lesotho and implications for correlations within the Karoo igneous province. In: Mahoney, J.J., Coffin, M.F. (Eds.), *Large Igneous Provinces: continental, Oceanic, and Planetary Flood Volcanism*. Am. Geophys. Union Geophys. Monogr., vol. 100, pp. 247–272.
- Melluso, L., Beccaluva, L., Brotzu, P., Gregnanin, A., Gupta, A.K., Morbidelli, L., Traversa, G., 1995. Constraints on the mantle sources of the Deccan Traps from the petrology and geochemistry of the basalts of Gujarat State (Western India). *J. Petrol.* 36, 1393–1432.
- Melluso, L., Barbieri, M., Beccaluva, L., 2004. Chemical evolution, petrogenesis, and regional chemical correlations of the flood basalt sequence in the central Deccan Traps, India. In: Pande, K., Sheth, H.C. (Eds.), *Magmatism in India through Time*. Proc. Indian Acad. Sci. (Earth Planet. Sci.), vol. 113, pp. 587–603.
- Melluso, L., Morra, V., Brotzu, P., Tommasini, S., Renna, M.R., Duncan, R.A., Franciosi, L., d'Amelio, F., 2005. Geochronology and petrogenesis of the Cretaceous Antampombato–Ambatovy complex and associated dyke swarm, Madagascar. *J. Petrol.* 46, 1963–1996.
- Melluso, L., Mahoney, J.J., Dallai, L., 2006. Mantle sources and crustal input in Mg-rich Deccan Trap basalts from Gujarat (India). *Lithos* 89, 259–274.

- Middlemost, E.A.K., 1989. Iron oxidation ratios, norms and the classification of volcanic rocks. *Chem. Geol.* 77, 19–26.
- Miller, J.A., Harris, C., 2007. Petrogenesis of the Swaziland and Northern Natal rhyolites of the Lebombo rifted volcanic margin, Southeast Africa. *J. Petrol.* 48, 185–218.
- Mitchell, C.H., Widdowson, M., 1991. A geological map of the southern Deccan Traps, India and its structural implications. *J. Geol. Soc. Lond.* 148, 495–505.
- Pande, K., 2002. Age and duration of the Deccan Traps, India: a review of radiometric and palaeomagnetic constraints. *Proc. Ind. Acad. Sci. (Earth Planet. Sci.)* 111, 115–123.
- Peate, D.W., 1997. The Paraná-Etendeka province. In: Mahoney, J.J., Coffin, M.F. (Eds.), *Large Igneous Provinces: continental, Oceanic, and Planetary Flood Volcanism*. Am. Geophys. Union Geophys. Monogr., vol. 100, pp. 217–245.
- Peng, Z.X., Mahoney, J.J., 1995. Drillhole lavas in the Deccan Traps and the evolution of the Réunion hotspot mantle. *Earth Planet. Sci. Lett.* 134, 169–185.
- Peng, Z.X., Mahoney, J.J., Hooper, P.R., Harris, C., Beane, J.E., 1994. A role for lower continental crust in flood basalt genesis? Isotopic and incompatible element study of the lower six formations of the western Deccan Traps. *Geochim. Cosmochim. Acta* 58, 267–288.
- Peng, Z.X., Mahoney, J.J., Hooper, P.R., Macdougall, J.D., Krishnamurthy, P., 1998. Basalts of the northeastern Deccan Traps, India: isotopic and elemental geochemistry and relation to southwestern Deccan stratigraphy. *J. Geophys. Res.* 103, 29843–29865.
- Peucat, J.J., Vidal, P., Bernard-Griffiths, J., Condie, K.C., 1989. Sr, Nd and Pb isotopic systematics in the Archaean low- to high-grade transition zone of southern India: Syn-accretion vs. post-accretion granulites. *J. Geol.* 97, 537–550.
- Ray, R., Sheth, H.C., Mallik, J., 2007. Structure and emplacement of the Nandurbar-Dhule mafic dyke swarm, Deccan Traps, and the tectonomagmatic evolution of flood basalts. *Bull. Volcanol.* 69, 531–537.
- Rollinson, H.R., 1993. *Using Geochemical Data: Evaluation, Presentation, Interpretation*. Longman, Harlow, UK (pp. 352).
- Sethna, S.F., Czygan, W., Sethna, B.S., 1987. Iron-titanium oxide geothermometry for some Deccan Trap tholeiitic basalts, India. *J. Geol. Soc. Ind.* 29, 483–488.
- Sheth, H.C., 2005. Were the Deccan flood basalts derived in part from ancient oceanic crust within the Indian continental lithosphere? *Gond. Res.* 8, 109–127.
- Sheth, H.C., 2006. The emplacement of pahoehoe lavas on Kilauea and in the Deccan Traps. *J. Earth Syst. Sci.* 115, 615–629.
- Sheth, H.C., Ray, J.S., 2002. Rb/Sr-<sup>87</sup>Sr/<sup>86</sup>Sr variations in Bombay trachytes and rhyolites (Deccan Traps): Rb–Sr isochron, or AFC process? *Int. Geol. Rev.* 44, 624–638.
- Sheth, H.C., Torres-Alvarado, I.S., Verma, S.P., 2002. What is the “calc-alkaline rock series”? *Int. Geol. Rev.* 44, 686–701.
- Sheth, H.C., Mahoney, J.J., Chandrasekharam, D., 2004a. Geochemical stratigraphy of flood basalts of the Bijasan Ghat section, Satpura Range, India. *J. Asian Earth Sci.* 23, 127–139.
- Sheth, H.C., Mathew, G., Pande, K., Mallik, S., Jena, B., 2004b. Cones and craters on Mount Pavagadh, Deccan Traps: rootless cones?. In: Sheth, H.C., Pande, K. (Eds.), *Magmatism in India through Time*. *Proc. Ind. Acad. Sci. (Earth Planet. Sci.)*, vol. 113, pp. 831–838.
- Shukla, A.D., Bhandari, N., Kusumgar, S., Shukla, P.N., Ghevariya, Z.G., Gopalan, K., Balaram, V., 2001. Geochemistry and magnetotratigraphy of Deccan flows at Anjar, Kutch. *Proc. Ind. Acad. Sci. (Earth Planet. Sci.)* 110, 111–132.
- Sreenivasa Rao, M., Reddy, N.R., Subbarao, K.V., Prasad, C.V.R.K., Radhakrishnamurthy, C., 1985. Chemical and magnetic stratigraphy of parts of Narmada region, Deccan basalt province. *J. Geol. Soc. Ind.* 26, 617–639.
- Stormer Jr., J.C., Nicholls, J., 1978. XLFrac: a program for interactive testing of magmatic differentiation models. *Comput. Geosci.* 4, 143–159.
- Subbarao, K.V., Hooper, P.R. (Compilers), 1988. Reconnaissance map of the Deccan Basalt Group in the Western Ghats, India. In: Subbarao, K.V. (Ed.), *Deccan Flood Basalts*. *Geol. Soc. Ind. Mem.*, vol. 10, (enclosure).
- Sun, S.-s., McDonough, W.F., 1989. Chemical and isotopic systematics of oceanic basalts: implications for mantle composition and processes. In: Saunders, A.D., Norry, M.J. (Eds.), *Magmatism in the Ocean Basins*. *Geol. Soc. Spec. Publ.*, vol. 42, pp. 313–345.
- Vanderkluyzen, L., Mahoney, J.J., Hooper, P.R., Sheth, H.C., Ray, R., 2006. Location and geometry of the Deccan Traps feeder system inferred from dyke geochemistry. *Eos Trans. AGU*, 87(52), Fall Meet. Suppl., Abstract V13B-0681.
- Verma, R.K., Mittal, G.S., 1974. Palaeomagnetic study of a vertical sequence of Traps from Mount Pavagarh, Gujarat, India. *Phys. Earth Planet. Inter.* 8, 63–74.
- Verma, S.P., Torres-Alvarado, I.S., Sotelo-Rodriguez, Z.T., 2002. SINCLAS: standard igneous norm and volcanic rock classification system. *Comput. Geosci.* 28, 711–715.
- Watson, E.B., Green, T.H., 1981. Apatite/liquid partition coefficients for the rare earth elements and strontium. *Earth Planet. Sci. Lett.* 56, 405–421.
- Wensink, H., 1987. Comments on “Deccan flood basalts at the Cretaceous/Tertiary boundary?” by V. Courtillot et al. *Earth Planet. Sci. Lett.* 85, 326–328.
- West, W.D., 1958. The petrography and petrogenesis of forty-eight flows of Deccan Trap penetrated by borings in western India. *Trans. Nat. Inst. Sci.* 4, 1–56.
- Widdowson, M., Cox, K.G., 1996. Uplift and erosional history of the Deccan Traps, India: evidence from laterites and drainage patterns of the Western Ghats and Konkan coast. *Earth Planet. Sci. Lett.* 137, 57–69.
- Widdowson, M., Pringle, M.S., Fernandez, O.A., 2000. A post K-T Boundary (Early Palaeocene) age for Deccan-type feeder dykes, Goa, India. *J. Petrol.* 41, 1177–1194.

**Sheth & Melluso 2008: Additional data tables not in the published paper**

**Table.** Selected feldspar analyses from the Pavagadh volcanic suite

feldspars		SiO <sub>2</sub>	Al <sub>2</sub> O <sub>3</sub>	FeO	CaO	Na <sub>2</sub> O	K <sub>2</sub> O	Sum	An%	Or%	Ab%
D81	C	51.96	30.03	0.69	12.65	3.98	0.33	99.6	62.5	1.9	35.6
D81	Int	65.09	19.88	0.32	1.16	5.60	7.91	100.0	5.6	45.5	48.9
D81	C	49.11	32.02	0.58	14.94	2.81	0.21	99.7	73.7	1.2	25.1
D81	R	49.90	31.37	0.61	14.24	3.19	0.22	99.5	70.2	1.3	28.5
D81	Gm	55.57	27.78	0.46	9.69	5.67	0.59	99.8	46.9	3.4	49.7
D97	Int	50.07	31.12	1.03	13.93	3.33	0.30	99.8	68.6	1.8	29.7
D97	Int	55.13	26.72	0.86	9.18	4.65	3.46	100.0	42.3	19.0	38.8
D97	Int	56.29	26.64	0.92	8.84	5.96	1.07	99.7	42.3	6.1	51.6
D97	Int	53.66	28.68	1.03	11.16	4.79	0.47	99.8	54.7	2.7	42.5
D97	C	51.26	30.64	0.64	13.38	3.63	0.33	99.9	65.8	1.9	32.3
D97	R	58.38	25.00	0.72	7.00	6.35	2.09	99.5	33.4	11.9	54.8
D97	Int	54.90	27.53	1.43	9.93	5.39	0.50	99.7	49.0	2.9	48.1
D97	Int	51.23	30.67	0.65	13.38	3.65	0.30	99.9	65.8	1.8	32.5
D79	Mic	52.30	29.91	0.70	12.58	4.06	0.33	99.9	61.9	1.9	36.2
D79	Mic	49.59	31.21	1.13	14.11	3.28	0.24	99.6	69.4	1.4	29.2
D79	Mic	63.85	20.86	0.32	2.35	6.11	6.05	99.5	11.4	35.0	53.6
D79	Mic	51.75	29.90	0.86	12.66	3.96	0.34	99.5	62.6	2.0	35.4
D79	Mic	53.97	28.71	0.88	10.99	5.07	0.25	99.9	53.7	1.5	44.8
D79	Mic	57.62	26.04	0.56	8.06	6.28	0.98	99.5	39.1	5.7	55.2
D79	Mic	64.94	19.81	0.29	1.23	4.79	8.95	100.0	6.0	51.8	42.2
D79	Mic	63.00	21.63	0.48	3.06	6.09	5.57	99.8	14.8	32.0	53.2
D79	Mic	64.92	19.72	0.41	1.29	5.01	8.64	100.0	6.2	49.8	43.9
D89	C	59.08	25.35	0.33	7.07	6.87	1.08	99.8	34.0	6.2	59.8
D89	M	58.45	25.80	0.37	7.69	6.58	1.01	99.9	37.0	5.8	57.2
D89	R	59.63	25.00	0.39	6.67	7.06	1.17	99.9	32.0	6.7	61.3
D89	Mic	59.17	25.11	0.39	6.64	6.91	1.36	99.6	32.0	7.8	60.2
D89	C	57.71	26.48	0.34	8.38	6.32	0.79	100.0	40.4	4.5	55.1
D89	C	59.20	25.30	0.33	6.92	6.98	1.14	99.9	33.1	6.5	60.4
D89	C	60.48	24.45	0.33	5.94	7.29	1.52	100.0	28.4	8.6	63.0
D89	C	59.39	25.10	0.37	7.11	6.90	1.05	99.9	34.1	6.0	59.9
D89	C	59.13	25.44	0.35	7.25	6.81	0.98	100.0	35.0	5.6	59.4
D89	C	57.85	26.29	0.40	8.29	6.30	0.79	99.9	40.2	4.6	55.3
D89	R	64.03	21.13	0.55	2.49	7.21	4.17	99.6	12.1	24.2	63.6

Note: C = core of phenocryst; R = rim of phenocryst; Int = interstitial; Gm = groundmass; Mic = microlite.

**Table.** Selected olivine analyses from the Pavagadh volcanic suite

Olivines		SiO <sub>2</sub>	FeO	MnO	MgO	CaO	Sum	Fo%	Fa%
D97	C	38.60	22.57	0.32	38.59	0.36	100.4	75.3	24.7
D97	R	37.23	27.61	0.48	33.95	0.33	99.6	68.7	31.3
D97	C	40.50	11.48	0.19	47.30	0.37	99.8	88.0	12.0
D97	R	37.81	25.41	0.48	36.00	0.33	100.0	71.6	28.4
D97	C	39.91	12.95	0.18	46.29	0.35	99.7	86.4	13.6
D81	C	38.98	17.56	0.26	42.04	0.38	99.2	81.0	19.0
D81	R	39.30	17.16	0.28	42.72	0.38	99.8	81.6	18.4
D81	C	39.90	14.16	0.2	45.21	0.34	99.8	85.1	14.9
D79	C	35.40	38.16	0.49	25.6	0.29	99.9	54.5	45.5
D79	Mic	34.65	40.26	0.64	23.35	0.23	99.1	50.8	49.2
D79	C	35.52	36.88	0.58	26.3	0.31	99.6	56.0	44.0
D79	R	35.59	38.08	0.62	25.87	0.24	100.4	54.8	45.2
D79	Mic	35.10	38.84	0.53	24.82	0.21	99.5	53.2	46.8
D79	Mic	34.56	41.96	0.73	22.21	0.26	99.7	48.5	51.5
D79	Mic	36.01	34.43	0.48	28.47	0.36	99.8	59.6	40.4
D79	Mic	35.11	39.58	0.75	24.27	0.26	100.0	52.2	47.8
D79	R	34.50	41.24	0.67	22.59	0.23	99.2	49.4	50.6
D79	Mic	34.76	41.42	0.69	22.89	0.18	99.9	49.6	50.4
D79	C	36.26	32.62	0.55	29.94	0.34	99.7	62.1	37.9
D79	R	36.23	34.49	0.58	27.88	0.39	99.6	59.0	41.0
D79	C	35.66	37.97	0.62	25.38	0.28	99.9	54.4	45.6
D89	C	32.46	54.59	1.71	11.75	0.29	100.8	27.7	72.3
D89	R	32.33	54.88	1.81	11.34	0.31	100.7	26.9	73.1
D89	R	32.16	54.81	1.85	11.12	0.32	100.3	26.6	73.4
D89	C	32.00	53.81	1.72	11.57	0.28	99.4	27.7	72.3
D89	R	32.14	54.36	1.79	11.38	0.33	100.0	27.2	72.8

**Table.** Selected pyroxene analyses from the Pavagadh volcanic suite

pyroxenes		SiO <sub>2</sub>	TiO <sub>2</sub>	Al <sub>2</sub> O <sub>3</sub>	FeO	MnO	MgO	CaO	Na <sub>2</sub> O	Cr <sub>2</sub> O <sub>3</sub>	Sum	Ca%	Fe*%	Mg%	Mg#
D81	C	49.96	1.01	3.64	5.37	0.13	15.96	22.38	0.18	0.53	99.16	45.8	8.8	45.4	83.8
D81	R	50.45	1.55	1.99	10.83	0.34	13.31	21.02	0.30		99.79	43.6	18.0	38.4	68.0
D81	Int	49.04	2.40	3.79	9.76	0.26	12.65	21.28	0.37		99.55	45.6	16.7	37.7	69.2
D81	Int	48.24	2.23	2.66	15.80	0.39	8.55	20.84	0.72		99.43	45.9	27.8	26.2	48.5
D81	Int	48.55	2.27	2.59	15.61	0.39	8.64	20.72	0.76		99.53	45.8	27.5	26.6	49.0
D81	C	50.26	1.29	3.03	7.23	0.16	15.06	21.89	0.24	0.13	99.29	45.0	11.8	43.1	78.4
D81	R	51.39	1.24	2.94	6.88	0.17	15.06	21.92	0.21	0.10	99.91	45.3	11.4	43.3	79.2
D81	M	50.07	1.08	3.70	5.63	0.13	15.65	22.07	0.25	0.66	99.24	45.7	9.3	45.0	82.9
D81	R	50.47	1.55	1.99	10.83	0.34	13.31	21.03	0.30		99.82	43.6	18.0	38.4	68.0
D81	R	48.69	1.82	3.88	9.51	0.20	14.06	20.93	0.26	0.09	99.44	43.5	15.7	40.7	72.1
D82	Mic	49.94	1.43	3.57	6.49	0.14	15.11	22.10	0.26	0.44	99.48	45.8	10.7	43.5	80.2
D82	C	50.56	1.33	3.44	6.02	0.13	15.69	21.94	0.19	0.17	99.47	45.2	9.9	44.9	82.0
D82	R	45.69	2.94	7.21	8.06	0.17	12.89	21.59	0.35	0.34	99.24	47.0	14.0	39.0	73.6
D82	Gm	50.41	1.49	3.46	7.11	0.15	15.40	21.36	0.16	0.29	99.83	44.1	11.7	44.2	79.1
D82	Gm	47.86	2.41	5.26	7.86	0.17	13.76	21.61	0.23	0.26	99.42	46.0	13.3	40.7	75.3
D97	C	52.46	0.65	2.31	4.27	0.11	16.45	22.42	0.23	1.01	99.91	46.0	7.0	47.0	87.0
D97	R	51.04	1.29	2.50	7.94	0.19	15.11	20.91	0.23	0.24	99.45	43.3	13.1	43.5	76.8
D97	R	51.84	1.04	2.65	6.36	0.16	15.88	21.29	0.23	0.43	99.88	43.9	10.5	45.6	81.3
D97	C	50.87	1.24	3.35	7.06	0.17	15.23	21.02	0.27	0.44	99.65	43.9	11.8	44.3	79.0
D97	R	50.22	1.91	3.18	8.82	0.21	14.26	20.89	0.28		99.77	43.7	14.7	41.5	73.8
D97	Int	48.13	3.03	4.02	10.57	0.31	13.01	20.04	0.37		99.48	43.0	18.2	38.8	68.1
D97	Int	50.94	1.61	2.51	10.34	0.29	14.76	19.21	0.23		99.89	40.0	17.2	42.7	71.2
D97	Int	51.41	1.23	1.71	9.49	0.32	14.57	20.48	0.26		99.47	42.3	15.8	41.9	72.6
D79	C	51.37	1.51	1.86	9.32	0.26	14.84	20.25	0.32		99.73	41.9	15.4	42.7	73.4
D79	C	48.52	2.65	3.90	8.98	0.17	14.08	20.93	0.38		99.61	43.9	15.0	41.1	73.3
D79	R	48.53	2.31	3.59	10.41	0.25	13.54	20.40	0.42		99.45	42.9	17.5	39.6	69.4
D79	R	48.20	2.64	4.03	9.66	0.14	13.40	20.86	0.41		99.34	44.2	16.2	39.5	70.9
D79	R	47.43	2.55	4.04	10.48	0.19	13.43	19.99	0.41		98.52	42.5	17.7	39.7	69.2
D79	R	48.08	2.38	3.98	10.03	0.21	13.60	20.56	0.40		99.24	43.3	16.8	39.9	70.3
D79	C	50.83	1.54	1.94	9.17	0.19	14.47	21.27	0.29		99.70	43.7	15.0	41.3	73.4
D79	C	47.71	2.52	4.24	9.37	0.13	13.39	21.38	0.40	0.02	99.16	45.1	15.6	39.3	71.5
D79	Mic	49.96	1.48	2.12	12.56	0.19	12.87	19.75	0.51		99.44	41.5	20.8	37.6	64.3
D79	Mic	48.49	2.17	3.55	9.75	0.15	13.48	21.19	0.39		99.17	44.4	16.2	39.3	70.8
D79	Mic	48.17	2.45	3.99	9.70	0.14	13.50	21.16	0.37		99.48	44.4	16.1	39.4	71.0
D89	C	50.41	0.48	1.02	18.64	0.81	10.74	17.57	0.19		99.86	36.8	31.7	31.3	49.6
D89	C	50.08	0.48	0.92	18.46	0.82	10.69	17.85	0.18		99.48	37.4	31.4	31.1	49.7
D89	R	51.39	0.35	0.93	18.93	0.93	9.50	17.18	0.59		99.80	37.4	33.6	28.8	46.0
D89	C	50.23	0.36	0.53	31.77	1.23	12.05	4.13	0.34		100.64	8.9	54.8	35.9	39.4
D89	C	50.29	0.40	0.93	19.56	0.78	10.49	16.96	0.25		99.66	35.8	33.3	30.8	47.9
D89	C	50.06	0.48	0.88	19.29	0.69	10.23	17.54	0.24		99.41	37.0	32.8	30.0	47.7
D89	R	49.76	0.47	0.97	20.17	0.78	10.11	16.60	0.27		99.13	35.3	34.6	29.9	46.2
D89	C	49.94	0.37	1.02	20.31	0.81	10.30	16.48	0.21		99.44	34.8	34.7	30.3	46.5
D89	R	50.33	0.35	0.83	19.94	0.82	10.18	17.06	0.23		99.74	36.0	34.0	29.9	46.6
D89	C	50.41	0.33	0.98	19.42	0.83	9.90	17.32	0.24		99.43	36.9	33.6	29.4	46.6
D89	R	50.41	0.45	0.85	19.40	0.34	10.01	17.94	0.22		99.62	37.9	32.5	29.5	47.5
D89	Gm	51.07	0.41	0.85	19.93	0.90	10.40	16.73	0.24		100.53	35.2	34.1	30.5	47.1
D89	Gm	51.20	0.34	0.81	20.10	0.81	9.52	15.72	0.54		99.04	34.7	35.9	29.2	44.8

**Table.** Selected biotite analyses from the Pavagadh volcanic suite

Biotites		SiO <sub>2</sub>	TiO <sub>2</sub>	Al <sub>2</sub> O <sub>3</sub>	FeO	MnO	MgO	CaO	Na <sub>2</sub> O	K <sub>2</sub> O	Sum
D79	Pec	41.50	4.36	11.80	9.01	0.09	20.79		0.85	9.67	98.10
D79	Pec	42.92	4.22	12.01	8.86	0.01	20.92		0.80	10.10	99.80

**Table.** Selected magnetite, ilmenite, and chrome-spinel analyses from the Pavagadh volcanic suite

<b>Magnetites</b>		TiO <sub>2</sub>	Al <sub>2</sub> O <sub>3</sub>	FeO	MnO	MgO	Cr <sub>2</sub> O <sub>3</sub>	Sum	Ulv	Fe <sup>II</sup>	Fe <sup>III</sup>	Ti
D79	Int	21.39	2.22	72.30	1.19	0.98		98.10	0.591	53.3	25.6	21.0
D79	Int	24.49	2.29	69.76	1.22	1.05		98.80	0.673	56.2	19.8	24.0
D89	Int	25.74	1.40	71.78	0.79	1.01		100.70	0.698	56.6	19.0	24.4
D89	Int	24.75	1.64	72.49	0.92	0.87		100.70	0.671	55.9	20.6	23.5
D89	Int	22.58	1.34	74.47	1.01	0.74		100.10	0.615	53.8	24.8	21.4
<b>Ilmenites</b>		TiO <sub>2</sub>	Al <sub>2</sub> O <sub>3</sub>	FeO	MnO	MgO	Cr <sub>2</sub> O <sub>3</sub>	Sum	ilm			
D79	Int	49.76	0.19	46.27	0.64	3.56		100.40	0.911			
D79	Int	49.44	0.15	46.89	0.64	3.31		100.40	0.906			
D79	Int	49.17	0.04	45.40	0.49	3.48		98.60	0.918			
D79	Int	48.46	0.12	46.29	0.49	3.01		98.40	0.909			
D97	Int	48.15		47.11	0.62	2.85		98.70	0.901			
D97	Int	49.60		46.52	0.57	2.83		99.50	0.922			
<b>Cr-spinels</b>		TiO <sub>2</sub>	Al <sub>2</sub> O <sub>3</sub>	FeO	MnO	MgO	Cr <sub>2</sub> O <sub>3</sub>	Sum				
D82	in ol	9.88	10.66	52.67	0.44	7.45	19.08	100.20	66.7	25.0		
D82	in ol	4.93	15.45	43.91	0.43	8.00	28.66	101.40	52.7	36.3		
D82	in ol	11.69	5.17	53.10	0.66	5.09	25.98	101.70	72.1	35.0		
D97	in ol	1.54	11.27	33.95	0.43	5.55	46.61	99.40	46.1	62.6		
D97	in ol	3.83	7.92	42.72	0.49	4.90	38.40	98.30	57.3	52.9		

**Table.** Results of discriminant function analysis for the mafic lavas of Pavagadh

Sample	Location	Best match	<i>p</i>	RUN 1			Best match	<i>p</i>	RUN 2		
				M-dist	Fn 1	Fn 2			M-dist	Fn 1	Fn 2
D92	705 m	Mah	0.000	241	10.618	-2.220	Mah	0.000	165	8.059	2.340
D93	685 m	Mah	0.000	103	9.126	-2.379	Mah	0.000	136	8.066	2.676
D94	665 m	Mah	0.000	231	11.787	-1.893	Mah	0.000	137	8.014	2.483
D95	645 m	Mah	0.000	384	1.004	-9.038	Mah	0.000	314	12.309	0.012
D96	580 m	Mah	0.000	112	3.822	-6.250	Mah	0.000	96	8.882	-0.132
D97	565 m	Mah	0.000	116	10.156	1.672	Mah	0.000	86	4.139	3.177
D98	480 m	Mah	0.000	126	5.366	-5.247	Mah	0.000	184	8.846	0.465
D157	390 m	-	-	-	-	-	-	-	-	-	-
D158	390 m	Mah	0.000	224	-0.299	-5.189	Mah	0.000	105	8.604	2.929
D159	355 m	Mah	0.000	181	-0.379	-6.836	Mah	0.000	113	9.411	0.984
D160	325 m	Mah	0.000	175	9.480	-0.205	Mah	0.000	151	3.171	0.562
D79	NWP	Mah	0.000	124	7.885	0.427	Mah	0.000	133	5.319	3.488
D81	NWP	Neral	0.000	96	8.769	1.305	Mah	0.000	75	3.411	2.476
D80	NWP	Mah	0.000	314	5.171	-10.150	Mah	0.000	416	10.121	-4.853
D85	NP	Mah	0.000	625	5.506	-10.235	Mah	0.000	674	10.391	-5.334
D84	NP	Mah	0.000	609	2.665	-13.045	Mah	0.000	524	16.110	-2.008
D82	NP	-	-	-	-	-	-	-	-	-	-
D83	NP	Mah	0.000	181	8.048	-6.922	Mah	0.000	226	11.410	-0.196

Notes: *p* = probability; M-dist = Mahalanobis distance; Mah = Mahabaleshwar Formation. Discriminant function analysis was carried out twice, with the following variables: RUN 1: SiO<sub>2</sub>, Al<sub>2</sub>O<sub>3</sub>, Fe<sub>2</sub>O<sub>3</sub>, FeO, CaO, MgO, K<sub>2</sub>O, P<sub>2</sub>O<sub>5</sub>, Ni, V, Ba, Rb, Sr, Zr, Y, Nb; RUN 2: Ni, V, Ba, Rb, Sr, Zr, Y, Nb. No results were obtained for D157 and D82 because data are not available for some of these elements.